Journal of Hydrology 367 (2009) 200–216

Contents lists available at ScienceDirect

Journal of Hydrology

journal homepage: www.elsevier.com/locate/jhydrol

A spatially explicit hydro-ecological modeling framework (BEPS-TerrainLab V2.0): Model description and test in a boreal ecosystem in Eastern North America

Ajit Govind [a,b,*], Jing Ming Chen [a], Hank Margolis [c,d], Weimin Ju [e], Oliver Sonnentag [f], Marc-André Giasson [c,d]

[a] Department of Geography, University of Toronto, 100 George Street, Room 5047, Toronto, Ontario, Canada
[b] Department of Forest Ecosystems and Society, Oregon State University, OR, USA
[c] Faculté de Foresterie et Géomatique, Université Laval, Québec, Canada
[d] Centre d'Étude de la Forêt (CEF), Québec, Canada
[e] International Institute for Earth System Sciences, Nanjing University, China
[f] Department of Environmental Sciences, Policy and Management, University of California, Berkley, CA, USA

ARTICLE INFO

Article history:
Received 22 February 2008
Received in revised form 13 December 2008
Accepted 9 January 2009

This manuscript was handled by P. Baveye, Editor-in-Chief, with the assistance of Magdeline Laba, Associate Editor.

Keywords:
Spatially explicit hydro-ecological model
Boreal ecosystems
Sub-surface baseflow
Gross primary productivity
Evapotranspiration

SUMMARY

A spatially explicit, process-based hydro-ecological model, BEPS-TerrainLab V2.0, was developed to improve the representation of ecophysiological, hydro-ecological and biogeochemical processes of boreal ecosystems in a tightly coupled manner. Several processes unique to boreal ecosystems were implemented including the sub-surface lateral water fluxes, stratification of vegetation into distinct layers for explicit ecophysiological representation, inclusion of novel spatial upscaling strategies and biogeochemical processes. To account for preferential water fluxes common in humid boreal ecosystems, a novel scheme was introduced based on laboratory analyses. Leaf-scale ecophysiological processes were upscaled to canopy-scale by explicitly considering leaf physiological conditions as affected by light and water stress. The modified model was tested with 2 years of continuous measurements taken at the Eastern Old Black Spruce Site of the Fluxnet-Canada Research Network located in a humid boreal watershed in eastern Canada. Comparison of the simulated and measured ET, water-table depth (WTD), volumetric soil water content (VSWC) and gross primary productivity (GPP) revealed that BEPS-TerrainLab V2.0 simulates hydro-ecological processes with reasonable accuracy. The model was able to explain 83% of the ET, 92% of the GPP variability and 72% of the WTD dynamics. The model suggests that in humid ecosystems such as eastern North American boreal watersheds, topographically driven sub-surface baseflow is the main mechanism of soil water partitioning which significantly affects the local-scale hydrological conditions.

Introduction

Hydrological controls on carbon (C) cycles and their implications on global climate change have recently gained attention in both modeling (e.g. Gedney et al., 2006; Betts et al., 2007) and measurement (e.g. Baldocchi et al., 1996; Verstraeten et al., 2006) studies. Many of these studies have demonstrated that there is a tight link between hydrological and C-cycling processes, with mechanisms operating differently at various spatio-temporal scales. There are several ecological processes that are highly sensitive to hydrological controls such as photosynthesis (Wang et al., 2001; Ju and Chen, 2005; Zhou et al., 2006), respiration (Mcguire et al., 2000; Reichstein et al., 2003), redox-mediated methane production (Blodau et al., 2007; Zhuang et al., 2004), transport of dissolved organic carbon (Neff and Asner, 2001; Hornberger et al., 1994), phenological dynamics such as Leaf Area Index (Band et al., 1993) and water use efficiency (Yu et al., 2004; Winner et al., 2004). Hydrological controls, thus, significantly affect many of the biogeochemical processes. However, the extent to which these interactions are relevant and their implications on the terrestrial C balance under climate change in different ecosystems is still an open question (e.g. Cox et al., 2000; Friedlingstein et al., 2006; Gedney et al., 2006).

Current understanding of biogeochemical processes of boreal ecosystems is inadequate due to their unique hydrological processes (Price et al., 1997; Devito et al., 1997, 2005). This topic is crucial in a climate change context because issues such as melting of permafrost and other forms of alterations in hydrological processes in high latitude boreal ecosystems could significantly affect its ecological and biogeochemical processes (Deming, 1995; Zimov et al., 2006). Only a handful of hydro-ecological modeling works have been conducted in the boreal eco-

* Corresponding author. Address: Department of Geography, University of Toronto, 100 George Street, Room 5047, Toronto, Ontario, Canada M5S 3G3. Tel.: +1 416 946 7715; fax: +1 416 946 3886.
E-mail addresses: ajit.govind@utoronto.ca, ajit.govind@oregonstate.edu (A. Govind).

0022-1694/$ - see front matter © 2009 Elsevier B.V. All rights reserved.
doi:10.1016/j.jhydrol.2009.01.006

systems although measurement oriented studies are common. This warrants the need for a boreal-specific hydro-ecological model having a systems approach which can explain the feedback mechanisms and interactions between the hydrological, ecophysiological and biogeochemical processes.

At the landscape scale, topographical differences control lateral water movement. This clearly indicates the importance of landscape-scale hydrological processes in controlling the local-scale water balance and hence, on the ecophysiological and biogeochemical processes. Current large-scale estimates of biogeochemical indicators overlook the large variations caused by topographic effects on soil water, temperature and nutrient availability (Grant, 2004; Kavvas et al., 2004, 2006). Hitherto, ecosystem modelers have been focusing either in capturing the point-scale intricacies (e.g., Grant et al., 2006; Ju et al., 2006) or large-scale generalizations (e.g., Ju and Chen, 2005; Turner et al., 2006) and often overlooked the strong hydro-ecological connections that are dominant at mesoscales (e.g. watershed-scale). Ecosystem modelers have been using different strategies to implicitly quantify hydrological controls on plant physiological mechanisms that determine various ecosystem responses. However, only a handful of models have explicitly bridged ecology and hydrology. Such studies have been carried out at point-scale (e.g. Grant et al., 2006; Ju et al., 2006; Daly et al., 2004; Porporato et al., 2003), watershed-scale (MacKay and Band, 1997; Tague and Band, 2004; Band et al., 2001); regional-scale (Liu et al., 1997; Potter et al., 2001; Coops et al., 2007) and global-scale (Hunt et al., 1996; Nemani et al., 2003). Although these studies have a coupled representation of ecological and hydrological processes, the coupling is not "tight" enough to comprehensively reveal the feedback relationships existing in the soil-plant-atmospheric continuum. Although, point-scale ecological models are generally comprehensive in terms of processes, they are limited in their ability to accommodate lateral hydrological processes to accurately explain the local-scale water balance of humid ecosystems.

Considering the research need, a spatially explicit hydro-ecological model, BEPS-TerrainLab V2.0 was developed that has a tighter coupling of hydrological, ecophysiological and biogeochemical processes focusing on boreal ecosystems. The main objective of this paper is to document BEPS-TerrainLab V2.0's boreal-specific conceptualizations and evaluate its performance by comparing various hydro-ecological simulations with measurements taken in a humid boreal landscape in eastern Canada.

Materials and methods

Model description

BEPS-TerrainLab V2.0 originated from the Boreal Ecosystem Productivity Simulator (BEPS, Liu et al., 1997) that was developed during the Boreal Ecosystem–Atmosphere Study (BOREAS). BEPS describes several biophysical processes such as canopy radiative transfer and stomatal dynamics and ecophysiological processes such as gross primary productivity (GPP), evapotranspiration (ET) and autotrophic respiration for a monolayer canopy. Photosynthesis (as GPP) is modeled using a spatially and temporally upscaled version of the instantaneous leaf-scale biochemical model of Farquhar et al. (1980) using the scheme outlined in Chen et al. (1999). Ecosystem-scale ET is calculated using the Penman–Monteith leaf-scale model with a spatial upscaling similar to photosynthesis. BEPS however uses a simple parameterization (bucket model) to represent hydrological controls on the above-mentioned ecophysiological processes in order to simulate the fluxes of mass and energy across the soil–plant–atmosphere continuum in a spatially explicit manner.

BEPS-TerrainLab V1.0 (Govind et al., 2006; Chen et al., 2007) was an improvement with the inclusion of a distributed hydrological model, TerrainLab (Chen et al., 2005) that was coupled to BEPS. TerrainLab adopted concepts from the distributed hydrological model of Wigmosta et al. (1994) and it was tested in the Southern Study Area (SSA) of the BOREAS region to study the spatio-temporal variation of ET and soil moisture. El Maayar and Chen (2006) used TerrainLab to develop empirical spatial upscaling algorithms for ET. As a coupled version of BEPS and TerrainLab, Chen et al. (2007) used BEPS-TerrainLab V1.0 as a learning tool to understand the impact of landscape-scale topographic variations on primary production in the mountainous areas of China. BEPS-TerrainLab V1.0 was further modified to include peatland-specific parameterizations for studying the coupled water and C-cycling processes of the Mer Bleue bog in southern Ontario by Sonnentag et al. (2008). All of the above-mentioned studies were conducted during the growing season and the strong linkages between local hydrology and C-cycling were not explored in detail. Moreover, the existence of many modeling gaps in adequately representing boreal hydro-ecology led to further improvements and eventually led to the creation of BEPS-TerrainLab V2.0.

Most hydrological processes are explicitly described within a BEPS-TerrainLab V2.0 modeling unit. This facilitates adequate description of soil water regimes by solving a detailed water balance equation in a spatially explicit manner at daily time-steps. The modeling unit (Fig. 1) was initially designed to match with high-resolution remote sensing products. However, the model can be run at any spatial resolution by resampling the spatial input datasets.

Canopy hydrological processes

Precipitation is the only input of water at the watershed-scale. In BEPS-TerrainLab V2.0, precipitation is categorized as rain or snow using a prescribed air temperature threshold of 0 °C. Vegetation canopies intercept precipitation as a function of their interception storage capacity. Some portion of canopy-intercepted precipitation directly returns to the atmosphere as canopy sublimation (snow) or canopy evaporation (rain), depending on the meteorological conditions. Factors affecting evaporation are available energy, dryness of air and wind speed. The precipitation that is not intercepted, directly reaches the ground surface as through-fall. The remainder of the water on the canopy after evaporation or sublimation reaches the ground surface by stem-flow.

The next important canopy hydrological process is transpiration. Unlike evaporation, strong biological controls determine the magnitudes of transpired water manifested through the ambient stomatal resistances for water vapor transport. Transpiration occurs from both overstory and understory canopy layers. However, physiological and microclimatic conditions of the leaves located at various levels of canopy strongly influence the rates of transpired water. The processes of evaporation and transpiration are modeled using the Penman–Monteith (PM) equation using leaf or surface-specific net radiation, stomatal (or surface) and aerodynamic resistances. Canopy evaporation is also computed in a similar way by replacing stomatal resistances with a very low resistance term (Running and Coughlan, 1988). The total ecosystem-scale ET can be expressed as:

$$\begin{aligned} ET = {} & x_1 \cdot T_{o\,sun,sat} + x_2 \cdot T_{o\,sun,unsat} + x_3 \cdot T_{o\,shade,sat} + x_4 \\ & \cdot T_{o\,shade,unsat} + y_1 \cdot T_{u\,sat} + y_2 \cdot T_{u\,unsat} + S_{floor} + z_1 \cdot E_{moss} \\ & + z_2 \cdot E_{soil} + I_{evap} + I_{sub} \end{aligned} \quad (1)$$

ET	Total ecosystem-scale evapotranspiration.
$T_{o\,sun,unsat}$	Transpiration from sunlit-overstory leaves getting unsaturated soil moisture.
$T_{o\,sun,sat}$	Transpiration from sunlit-overstory leaves getting saturated soil moisture.
$T_{o\,shade,unsat}$	Transpiration from shaded-overstory leaves getting unsaturated soil moisture.
$T_{o\,shade,sat}$	Transpiration from shaded-overstory leaves getting saturated soil moisture.
$T_{u\,unsat}$	Transpiration from understory leaves getting unsaturated soil moisture.
$T_{u\,sat}$	Transpiration from understory leaves getting saturated soil moisture.
S_{floor}	Sublimation of snow from forest-floor.
E_{moss}	Evaporation from the moss surface.
E_{soil}	Evaporation from the soil surface.
I_{evap}	Evaporation of water intercepted on canopy.
I_{sub}	Sublimation of snow intercepted on canopy.
x_{1-4}	Overstory transpiration upscaling factors for various light and moisture regimes.
y_{1-2}	Understory transpiration weighting factors for moisture regimes.
z_{1-2}	Forest-floor evaporation weighting factors for soil or moss fractions.

Each of the ET sub-component (except sublimation) is calculated using the Penman–Monteith equation expressed in a general form as given below:

$$Ex = \frac{\Delta R_{nx} + \rho c_p \frac{e_s - e}{\alpha}}{\lambda_v\left(\Delta + \gamma\left(1 + \frac{\beta}{\alpha}\right)\right)}\delta t \tag{2}$$

Ex is the amount of water evaporated or transpired from a unit surface, x (leaf, moss or a soil patch). R_{nx} is the net radiation available on the evaporating or transpiring surface, see Chen et al. (2005) for equations. ρ is the density of moist air, calculated as a function of air temperature. C_p is the specific heat of air at a constant pressure. e_s and e are the saturated and actual vapor pressures, respectively. λ is the latent heat of vaporization of water, Δ is the slope of the saturated vapor pressure–temperature curve, γ is the psychrometric constant, a weak function of ambient air temperature, α is the aerodynamic resistance for a given canopy layer; and β is the stomatal (or surface) resistance for a given leaf or soil-surface under a given light and moisture regime.

$\beta = 0$ when $x = I_{evap}$.	
$\beta = r_{s\ sun,unsat}$	The stomatal resistance of sunlit-overstory leaves, when $x = T_{o\ sun,unsat}$.
$\beta = r_{s\ sun,sat}$	The stomatal resistance of sunlit-overstory leaves, when $x = T_{o\ sun,sat}$.
$\beta = r_{s\ shade,unsat}$	The stomatal resistance of shaded-overstory leaves, when $x = T_{o\ shade,unsat}$.
$\beta = r_{s\ shade,sat}$	The stomatal resistance of shaded-overstory leaves, when $x = T_{o\ shade,sat}$.
$\beta = r_{c\ under\ unsat}$	The canopy resistance of the understory when $x = T_{u\ unsat}$.
$\beta = r_{c\ undersat}$	The canopy resistance of the understory when $x = T_{u\ sat}$.
$\beta = r_{soil/moss}$	The soil or moss resistance as a function of VSWC when $x = E_{floor}$.

In all the cases, β for water vapor transport is calculated as the reciprocal of total stomatal conductance ($g_{s,t}$) which is calculated using the Jarvis algorithm (see the Appendix A). Unlike BEPS-TerrainLab V1.0, where constant values for aerodynamic resistances (α) were used irrespective of the vertical position of the evapotranspiring surface (overstory, understory or forest-floor), BEPS-TerrainLab V2.0 explicitly calculates α for different canopy layers using the approach given by Tague and Band (2004). A logarithmic wind speed decay profile is assumed for the top of the overstory canopy and an exponential wind speed decay profile is assumed within the canopy.

Forest-floor evaporation

Forest-floor ET (E_{floor}) is the sum of moss and soil evaporation. Separation of soil and moss evaporation is complicated because the distribution of moss spatially varies quite rapidly at sub-pixel scales. To circumvent this issue, a land-cover specific moss cover fraction (ξ) is prescribed. Since the sum of the *area index* of soil and moss together is 1, no weighting term is necessary to spatially upscale E_{floor}.

$$E_{floor} = (E_{moss} \cdot \xi) + (E_{soil} \cdot (1 - \xi)) \tag{3}$$
$$E_{moss/soil} = f(R_{n\,floor}, g_{soil} : g_{moss})$$

Unsaturated zone hydrological processes

Conceptually, BEPS-TerrainLab V2.0 has two soil layers with regard to hydrological processes: the unsaturated and the saturated zones. The unsaturated zone is the region above the water-table depth (WTD), where the volumetric soil water content (VSWC) is below saturation. The water entering the soil surface as infiltration is comprised of through-fall, stem-flow and snowmelt water. The process of infiltration continues until an infiltration capacity, $I_{\max}$ is reached. $I_{\max}$ is calculated based on Beckers and Alila (2004). Above the infiltration capacity, water ponds and laterally flow as surface over-land flow (SOLF). Percolation and capillary rise are the vertical movements of water between the unsaturated and saturated zones. Water in the unsaturated zone having potential energy above the field capacity moves vertically downward under the influence of gravity and reaches the saturated zone. Percolation is calculated after Chen et al. (2005).

Capillary rise can occur from the saturated zone to the unsaturated zone under conditions of excessive surface dryness. This upward flux of water occurs against the gravity under conditions when unsaturated zone VSMC is well below saturation creating potential gradient in the upward direction. Capillary rise is modeled according to Eagleson (1978) as described in Chen et al. (2005). The unsaturated hydraulic conductivity (K_θ) and matric potential used for the calculation of percolation and capillary rise are obtained using pedo-transfer functions (Campbell and Norman, 1998).

Other forms of hydrological processes in the unsaturated zone include transpiration-losses via overstory and understory root-fractions that lie in the unsaturated zone. Forest-floor evaporation is yet another water loss from the unsaturated zone as described in the section, 'Forest-floor evaporation'. The average VSMC of the unsaturated zone is calculated as the ratio unsaturated zone storage, S (m) and water-table depth, WTD (m).

Saturated zone hydrological processes

Saturated zone accounts for the storage below the WTD (measured from the soil surface down to the point where the soil moisture is less than saturation). At a daily time step, the gains or losses of water in the saturated zone includes percolation of water from the unsaturated zone, capillary rise to the unsaturated zone, topographically driven lateral sub-surface baseflow, and transpiration-losses via overstory and understory root-fractions that lie in the

saturated zone. The topographically driven lateral sub-surface baseflow is modeled as described below.

$$Q_{baseflow} = \sum_{i=1}^{8} T_{ij} \cdot \beta \cdot w \quad (4)$$

where $Q_{baseflow}$ is the baseflow in $m^3\,day^{-1}$ and β is the local water-table slope (analogous to the hydraulic gradient). In BEPS-TerrainLab V2.0, the conventional topographic gradient is replaced with water-table gradient to explicitly represent the hydraulic gradient to suit boreal applications where surface topographical differences are subtle (Fig. 2). For a given pixel ij, the effective width of flow (w) is assumed to be $0.5x$ in the cardinal direction and $0.398x$ in the diagonal direction (Quinn et al., 1991), where x is the grid size. T_{ij} is the hydraulic transmissivity ($m^2\,day^{-1}$), which is calculated as shown below.

$$T_{ij} = K_{sat\,ij} \cdot \frac{(\exp^{-f_{ij} \cdot z_{ij}} - \exp^{-f_{ij} \cdot d_{ij}})}{f_{ij}} \quad (5)$$

where $K_{sat\,ij}$ is the saturated hydraulic conductivity, f is the K_{sat} – *depth* decay constant, z_{ij} is the WTD and d_{ij} is the depth of the soil profile. The net sub-surface baseflow of a given pixel is the difference between the total sub-surface inflow and total sub-surface outflow from the 8 neighboring pixels.

The above conceptualization alone is insufficient to yield realistic baseflow for boreal landscapes. This is mainly due to preferential water fluxes that occur through the moss-peat layer, commonly found on boreal forest-floors (Price et al., 1997). Moss-peat layer has macroporous conduits that facilitate preferential water fluxes. The importance of preferential flow in humid forest-floors has been recently recognized by both experimentalists and modelers (e.g., Beckers and Alila, 2004; Weiler and McDonnell, 2007). Currently, very few hydrological models consider preferential water fluxes in a spatially explicit manner. In BEPS-TerrainLab V2.0, it is conceptualized that as long as WTD remains below the peat layer, i.e. in the mineral soil, no preferential flow occurs, and baseflow is calculated in the conventional manner using a

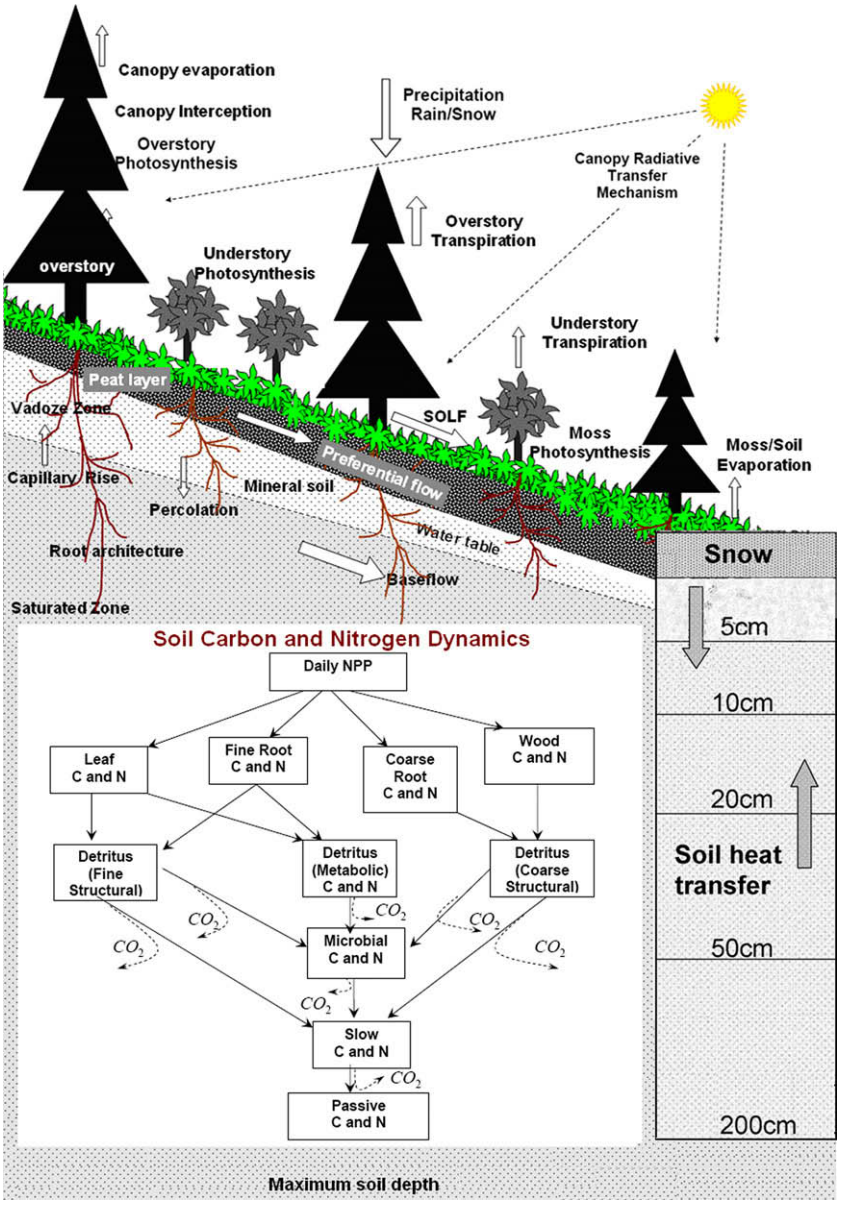

Fig. 1. A BEPS-TerrainLab V2.0 modeling unit where most of the boreal hydro-ecological processes are explicitly represented. The soil profile is divided into saturated and unsaturated zones by WTD. The lateral water fluxes that link neighboring pixels include sub-surface baseflow and SOLF that are topographically driven.

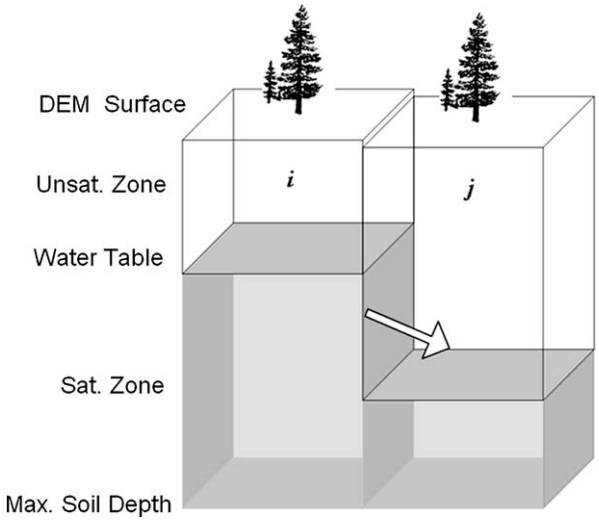

Fig. 2. Calculation of hydraulic head gradient using water-table slope. This approach seems to work well in boreal landscapes where the topographic differences are subtle.

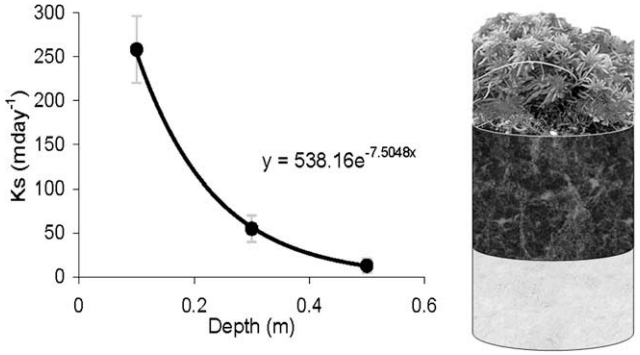

Fig. 3. Variation of saturated hydraulic conductivity (Ks_{peat}) with depth for a moss-peat system. This decay scheme is used to parameterize baseflow once the WTD reaches a land-cover specific "*peat layer criteria*". This procedure implicitly captures the preferential flow of water on boreal landscapes. A constant head permeameter approach was used to measure Ks_{peat} in the laboratory.

transmissivity value calculated according to Eq. (5). However, when the WTD reaches a *peat depth criteria*, z_p (land-cover-specific), the baseflow fluxes occur preferentially using a transmissivity (T_{peat}) which is calculated using a $K_{sat\,peat}$ – *depth* decay scheme as a function of peat saturated hydraulic conductivity, Ks_{peat}, and WTD (z_{ij}), as shown below.

$$T_{peat_{ij}} = \frac{K_{sat\,peat}(\exp^{-7.5048 z_{ij}} - \exp^{-7.5048 z_p})}{7.5048} \quad (6)$$

This parameterization was developed based on laboratory measurements of Ks_{peat} for several peat columns collected at different depths. In the summer of 2004, peat cores were collected from 5 locations in a boreal landscape, at three depths, i.e., 0–15 cm; 15–30 cm and 30–50 cm using aluminum cores 10 cm in diameter and 35 cm in length. Depth variation of Ks_{peat} was estimated using a constant head permeameter (See the Supplementary Video File). From this data, a curve was fitted to explain the variation of Ks_{peat} with depth, as shown in Fig. 3. The measurements revealed that the surface Ks_{peat} can be as high as as 258 ± 5 m day^{-1}and the $K_{sat\,peat}$ – *depth* decay constant was as high as 7.5048.

In BEPS-Terrainlab V2.0, once all the unsaturated and saturated zone hydrological components are calculated, the current day WTD is updated using fluctuations in water contents in the saturated and unsaturated zones.

Under conditions of excessive soil profile saturation, WTD can reach the soil surface and thereafter, any water that is added to the soil profile gets "ponded" which drains-off laterally as SOLF ($R_{surface}$). Although the occurrence of SOLF is rare in boreal forests due to high infiltration capacities associated with the moss-peat substratum, some ephemeral expressions of surface water fluxes can be found in low-lying areas of the watershed or during the spring snowmelt. In order to explicitly describe SOLF, a modified Manning's approach proposed by Voinov et al. (1998) is adopted in BEPS-Terrainlab V2.0. The ponded water in a given pixel is allowed to move laterally over the surface until it enters the water balance of the neighboring pixels.

The net water balance for a pixel can be summarized as:

$$\text{In the unsaturated zone, } \Delta W_{unsat} = P - S - I_{evap} - R_{surface} + W_{cr} - W_{pe} - T_{unsat} - E_{floor} \quad (7)$$

$$\text{In the saturated zone, } \Delta W_{sat} = W_{pe} - R_{baseflow} - T_{\mathrm{sat}} - W_{\mathrm{cr}} \quad (8)$$

Net water balance of the soil profile (pixel) as a whole is the sum of the storage changes in the unsaturated and saturated zones, which is determined by adding ΔW_{sat} and ΔW_{unsat}.

$$\Delta W = P - S - I_{evap} - R_{surface} - R_{baseflow} - T_{unsat} - T_{sat} - E_{floor} \quad (9)$$

Here ΔW is the storage change of a soil profile; P, the precipitation; S, all forms of sublimation; I_{evap}, all forms of canopy water evaporation; $R_{baseflow}$, the sub-surface baseflow; $R_{surface}$, the surface overland flow; T_{unsat}, the transpiration loss from the unsaturated zone (overstory + understory); T_{sat}, the transpiration loss from the saturated zone (overstory + understory); E_{floor}, the evaporation from the forest-floor (moss + soil); W_{pe}, the percolation from the unsaturated to saturated zone and W_{cr} is the capillary rise from the saturated to unsaturated zone.

Photosynthesis and ecosystem primary production

According to Farquhar et al. (1980), the process of photosynthesis for a C3 leaf at a given instant can be approximated as the minimum of rubisco-limited and light-limited gross photosynthetic rates as shown below.

$$A = \min(W_c, W_j) - R_d \quad (10)$$

$$\text{where } W_c = V_m \frac{C_i - \Gamma}{C_i + K} \quad \text{and} \quad W_j = J \frac{C_i - \Gamma}{4.5C_i + 10.5\Gamma} \quad (11)$$

A is the net photosynthesis, W_c and W_j are rubisco-limited and light-limited gross photosynthetic rates, respectively. R_d is the dark respiration. V_m is the maximum carboxylation rate. C_i is the intercellular CO_2 concentration; K is a function of enzyme kinetics. Γ is the CO_2 compensation point without the effects of dark respiration. Both Γ and K are temperature-dependent parameters (Chen et al., 1999). V_m is expressed as a function of both temperature and leaf nitrogen content (Bonan, 1995).

$$V_m = V_{m25} \cdot 2.4^{\frac{(T-25)}{10}} \cdot f(T) \cdot f(N) \quad (12)$$

In BEPS-TerrainLab V2.0, leaf nitrogen (N) is temporally varied by simulating the hydrologically controlled decomposition of soil organic matter and nitrogen mineralization (Govind et al., in press). This ensures that hydrology and biogeochemical processes are tightly coupled.

Chen et al. (1999) developed an analytical solution to temporally upscale (Eq. (10)). The temporally integrated model is adequate for daily GPP calculations because it preserves the physiological meaning of photosynthesis as well as mathematical consistency. The temporally integrated photosynthesis model of Chen et al. (1999) is strongly dependent on $g_{s,t}$, which in BEPS-Ter-

rainLab V2.0 is a strong function of the local-scale hydrological regimes and environmental factors. In addition, the hydrologically controlled biogeochemical processes affect plant nutrition which affects Eq. (12). These representations suggest that ecological, biogeochemical and hydrological processes are tightly coupled within BEPS-TerrainLab V2.0.

Site description

The model evaluation was conducted on a boreal landscape located near Chibougamau, North-central Quebec, Canada (Fig. 4). The Eastern Old Black Spruce site (EOBS) of the Fluxnet-Canada Research Network (FCRN) is located at 49.69°N and 74.34°W, which is ~50 km south-east of Lake Chibougamau and ~200 km northwest of Lac St. Jean. The climate of this region is cold temperate with a mean annual temperature of 0 °C and a mean annual precipitation of 961.3 mm (Environment Canada, 2006). The landscape has a rolling topography with a gentle slope of <5%, typical of the Canadian Shield. This gentle terrain represents glacial landform features. Since the soil is derived from glacio-fluvial deposits, it consists of poorly graded materials. Organic soils are composed mainly of moss necromass in poorly drained depressions and flat areas where black spruce trees dominate.

Fig. 4. Location of the Chibougamau watershed. The scale shown in the figure applies to the watershed.

The vegetation on this boreal landscape is dominated by black spruce (*Picea marina*) or aspen (*Populus* sp.). Jack pine (*Pinus banksiana*) and tamarack (*Larix larandicina*) occur sporadically. The understory is dominated by Labrador tea and the forest-floor consists of a thick moss dominated by feather moss and lichens in the moderately dry locations and *Sphagnum* sp. in wetter locations. At the landscape scale, vegetation varies across the gentle topographic gradient. On elevated parts of the landscape such as eskers, deciduous and mixed forests can be seen. On relatively flat and low-lying locations, there is a species transition from dense black spruce–moss dominated stands to wetlands dominated by moss and stunted black spruce trees.

Spatial data set preparation

Several spatially explicit input datasets are required to run BEPS-TerrainLab V2.0. Most of these datasets were prepared using a combination of remote sensing, geographic information system (GIS), ground measurements and modeling methods. Fig. 5A–F shows various spatial datasets used in this study. Since land-cover specific parameters are required to simulate ecophysiological and hydrological processes in a spatially explicit manner, a land-cover map was obtained from the Earth Observation for Sustainable Development of Forests, EOSD, a joint project between the Canadian Forest Service and the Canadian Space Agency. In 2005, a ground truth campaign was conducted and the EOSD land-cover product was confirmed to be of high quality. Table 1 shows some of the major land-cover specific biophysical parameters used in this study.

A digital elevation model (DEM) is required for topographic corrections of the daily meteorological variables and also for simulating the lateral hydrological processes. A DEM was obtained from the Canadian Council of Geomatics (CCG), which was further processed to make it hydrologically consistent. Since no watershed boundary was delineated for this location in previous studies, a watershed boundary was delineated from the hydrologically corrected DEM using a GIS (ArcGIS 9.1®). Routine watershed delineation procedures were performed using the D-8 flow scheme of Jenson and Domingue (1988). Since this boreal landscape has subtle topographic variations (376–415 masl), delineation of a watershed boundary was a challenge. Several flow-accumulation threshold values were tried to derive a watershed boundary that also retained the 1 km^2 footprint area of the Eddy covariance tower at the EOBS site. The topography-derived watershed drains into Lake Inlet located at its centre as shown in Fig. 5A–F. The unconventional shape of the watershed in the southern portion is because of the presence of a wetland (an ombotrophic bog) which is near-flat but located at a relatively higher elevation.

Because leaf abundance controls the interception of solar energy by vegetation and many of the canopy hydrological processes, spatially explicit information on Leaf Area Index (LAI) is required. A LAI map was obtained by combining remote sensing techniques and ground-based LAI measurements. A Landsat-TM image was used to derive a watershed-scale Normalized Difference Vegetation Index (NDVI) map. Further, LAI measurements taken along a 400 m transect (Chen et al., 2006) were correlated with corresponding NDVI values to derive a site-specific LAI–NDVI algorithm (Fig. 6). This algorithm was inverted using the NDVI map to derive watershed-scale LAI.

Information on soil texture is required to parameterize various soil hydraulic properties. Since very limited soil information exists at fine spatial resolutions for the study site, a watershed-scale soil texture map was derived using a look-up table procedure combining information on plot-scale soil textural analysis (Bernier et al., 2005), information on soil-surface deposit (Quebec Ministry of

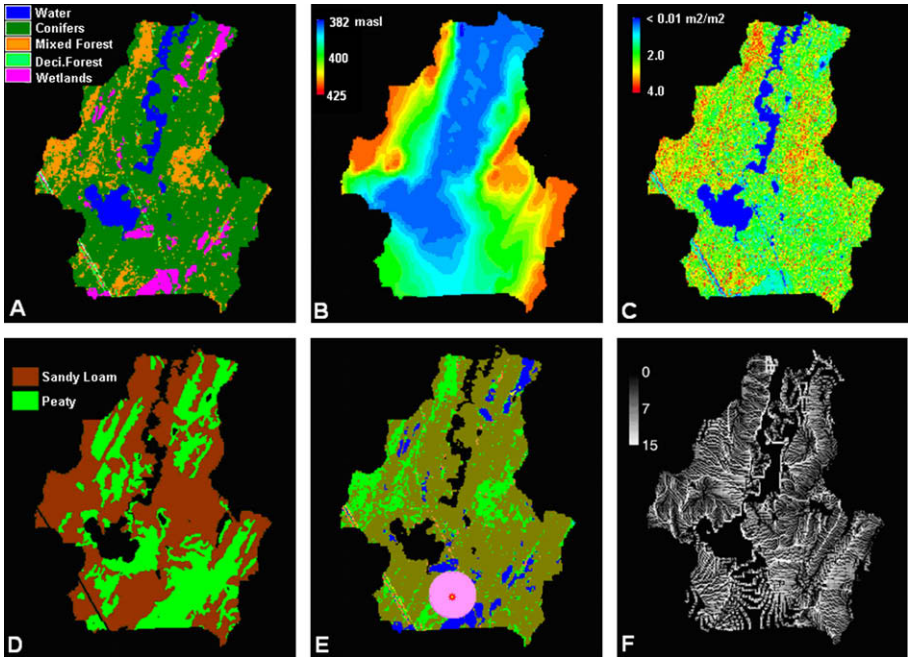

Fig. 5. Various spatial datasets required to run BEPS-TerrainLabV2.0 at a daily time-step. (A) A validated land-cover map. (B) Digital elevation model (DEM) that was further processed to make it hydrologically consistent. Aspect and slope were derived from the DEM. (C) Leaf area index (LAI) map derived using remote sensing and ground-based LAI measurements (D) Soil texture map. (E) The ~1 km^2 footprint of the EC tower and (F) Wetness Index used for a topography-based initialization of WTD. All the data sets have a spatial resolution of 25 × 25 m. Projection is UTM Zone 18 N. The scale of the ~40 km^2 watershed is shown in Fig. 4.

Table 1
Landcover specific biophysical parameters used in BEPS-TerrainLab V2.0.

Biological parameter	Units	Conifer	Mixed	Deciduous	Wetlands
Canopy clumping index	–	0.50[a]	0.70[a]	0.80[a]	0.90[b]
Maximum carboxylation rate at 25 °C	μmol m^{-2} s^{-1}	33.0[c]	50.0[d]	60.0[d]	33.0[c,e]
Maximum stomatal conductance	mm s^{-1}	1.60[a]	3.00[a]	5.00[a]	1.60[f]
Cuticular conductance	mm s^{-1}	0.15[g]	0.15[g]	0.15[g]	0.15[g]
Optimum temperature for photosynthesis	°C	20.0[h]	20.0[h]	20.0[h]	20.0[h]
Maximum temperature for photosynthesis	°C	37.0[h]	37.0[h]	37.0[h]	37.0[h]
Vapor pressure deficit at stomatal opening	kPa	0.20[i]	0.20[i]	0.20[i]	0.20[i]
Vapor pressure deficit at stomatal closure	kPa	2.00[i]	2.00[i]	2.00[i]	2.00[i]
Root extinction coefficient	–	0.94[j,k]	0.95[j,k]	0.96[j,k]	0.93[j]
Overstory canopy height	m	8.0[l,p]	10.0[p]	12.0[p]	3.0[p]
Understory canopy height	m	1.0[l,p]	2.0[p]	1.5[p]	0.5[p]
Wind attenuation coefficient	–	2.74[m,n,o]	2.78[m]	2.78[m]	2.74[m]
Moss fraction	%	85[p]	75[p]	50[p]	90[p]
Peat depth criteria	cm	20.0[p]	15.0[p]	15.0[p]	50.0[p]
Precipitation interception coefficient	mm LAI^{-1} day^{-1}	0.20[q,r]	0.25[q,r]	0.30[q]	0.10[q,r]

[a] Liu et al. (2002, 1997) and Chen et al. (2006).
[b] Sonnentag et al. (2007) and unpublished measurements at a wetland location near the EOBS site.
[c] Bonan (1995) and Chen et al. (1999).
[d] After Wilson et al. (2001).
[e] Wetlands in the study site have stunted black spruce trees.
[f] Sonnentag et al. (2008).
[g] This study.
[h] After Kimball et al. (1997), Chen et al. (1999) and Way and Sage (2008).
[i] Dang et al. (1997), Kimball et al. (1997) and Chen et al. (1999).
[j] After Jackson et al. (1996) for mixed forests, the value is calibrated between conifers and deciduous.
[k] After Chen et al. (2005).
[l] Fluxnet Canada-data information system.
[m] Amiro and Davis (1988).
[n] Cionco (1978).
[o] Heddeland and Lettenmaier (1995).
[p] Calibrated in this study, based on 2004 and 2005 field campaigns.
[q] Running and Coughlan (1988).
[r] Adjusted to account for the effects of leaf morphology on interception.

Natural Resources) and land-cover. USDA soil textural class in addition to a "peat" class was determined based on the look-up table procedure and spatially explicit hydraulic properties were assigned (Table 2).

Flux and meteorological measurements

Eddy covariance (EC) technique is being used to make continuous measurements of CO_2 and energy fluxes at the EOBS site. EC

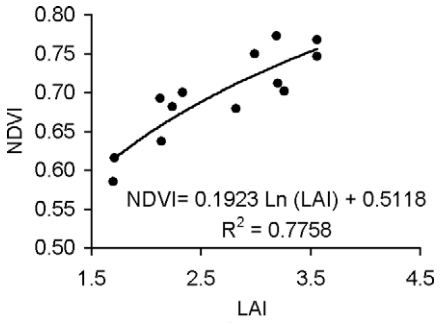

Fig. 6. NDVI–LAI algorithm developed using ground-based LAI measurements (taken along an east–west transect during the 2003 growing season) and remote sensing derived NDVI values. This algorithm was inverted and applied to the entire watershed to derive a watershed-scale LAI map.

instrumentation at EOBS comprises of a three-dimensional sonic anemometer and infrared gas analyzers (IRGA) mounted on a scaffold tower 24 m above the ground surface. Continuous meteorological measurements are also made on the EC tower. In the tower-footprint area, time domain reflectometers (Campbell Scientific CS615 sensor) are used to measure VSWC. Electronic piezometers (Solinst level-loggers) are used to monitor the fluctuations of WTD. Rainfall is measured using a tipping bucket rain gauge near the EOBS tower and the total precipitation is measured using a Geonor T200B rain gauge. More details on the measurements at the EOBS site can be found in Bergeron et al. (2007). Considering the tower height, prevailing wind direction and the gentle terrain, the tower footprint corresponds to an approximate circular shape having a radius of ~500 m centred on the tower.

Since BEPS-TerrainLab V2.0 runs at a daily time-step, half-hourly meteorological and flux measurements were temporally upscaled to a daily time-step for simulation and validation, respectively. All pixels in the watershed were assigned explicit meteorological data that were locally corrected for the effects of slope and elevation using a separate meteorological module within BEPS-TerrainLab V2.0. For the present study, meteorological measurements taken between January 2004 and December 2005 were used. To understand the spatio-temporal dynamics of plant growth and C-cycling, GPP was considered as the indicator in this study. The fluxes of net ecosystem exchange of carbon dioxide measured at the EC tower were partitioned to derive GPP by Bergeron et al. (2007) and this product was supplied through the FCRN's *Data Information System* which was directly used for model validation. The latent heat flux measurements (W m^{-2}) were converted to ET (mm day^{-1}) for model comparison.

Initialization of water-table depth, ecosystem carbon pools and model calibration

Initial WTD being a necessary input to BEPS-TerrainLab V2.0, an initial WTD was spun up before the actual simulation. To this end, the model was iteratively run several times using 2004 meteorological data. The first step in the iterative initialization procedure used a topography-derived WTD using the TOPMODEL principle of Beven and Kirkby (1979). Thereafter, the spun-up WTD was used for subsequent analyses. The WTD from DOY 365 of 2004 was used as the initial WTD for 2005 simulation.

BEPS-TerrainLab V2.0 requires information on the current sizes and C:N ratios of various ecosystem C-pools (13 in all) to run the biogeochemical processes that indirectly affect hydro-ecological processes. Ecosystem C-pools were initialized using a long-term model considering the historical variation in climate, variations in atmospheric CO_2 concentration, disturbance effects and temporal trends in N-deposition (Chen et al., 2003).

The model was calibrated for some of the parameters specific to boreal applications (see Table 1) using the GPP, ET, WTD and VSMC measurements for 2004. For the 2005, same parameter values as in 2004 were used. In this study, the 2004 simulations can be considered as a calibration year and 2005 as a validation year. Most of the other coefficients were already calibrated and validated in the predecessor models (Liu et al., 1997, 2002, 2003; Chen et al., 1999; Govind et al., 2006; Sonnentag et al., 2008) for boreal applications.

Results and discussion

Spatio-temporal patterns of ET

The simulated daily total ET fluxes (Eq. (1)) were compared to the ET derived from the latent heat fluxes measured at the EOBS tower site. Fig. 7a shows the seasonal patterns of the measured and the modeled ET for the footprint region for 2004 and 2005, respectively. Five-day moving averages of the simulated and measured ET for 2004 and 2005 are displayed for visual clarity. A one-to-one comparison of the daily values (Fig. 7b) were able to explain 82% (RMSE = 0.34 mm day^{-1}) and 84% (RMSE = 0.40 mm day^{-1}) of the variability in the measured ET in 2004 and 2005, respectively.

Although there is a general tendency of the model to underestimate ET, it seems to perform adequately for most parts of a year. Most of the discrepancies were found during winter, when the model underestimated the total ecosystem ET, especially in 2004. One possible explanation for this discrepancy is that snow sublimation might have contributed to higher winter latent heat values

Table 2
Hydraulic properties of various soil types in the watershed.

Hydraulic property	Symbol	Unit	Sandy loam	Peat
Field capacity	θ_{330}	%	0.33[a,d]	0.45[b]
Permanent wilting point	θ_{1500}	%	0.10[c,d]	0.10[b]
Porosity	φ	%	0.46[e,d]	0.83[e]
Max. conductance of soil surface	α	mm s^{-1}	1.0[f]	2.0[f]
Saturated hydraulic conductivity (vertical)	$K_{sat,vertical}$	m day^{-1}	6.0[b]	258[h]
Saturated hydraulic conductivity (horizontal)	$K_{sat,horizontal}$	m day^{-1}	10.0[b]	258[h]
Ks-decay rate with depth	σ	m^{-1}	0.03[f]	7.50[h]
Exponent of the moisture release equation	b	–	4.9[d,g]	6.0[i]

[a] Tombul et al. (2004).
[b] This study.
[c] Kirchmann et al. (1999).
[d] Rawls et al. (1982).
[e] Schwarzel et al. (2002).
[f] This study, calibrated.
[g] Beringer et al. (2001).
[h] This study, based on laboratory measurements of peat hydraulic properties.
[i] Letts et al. (2000).

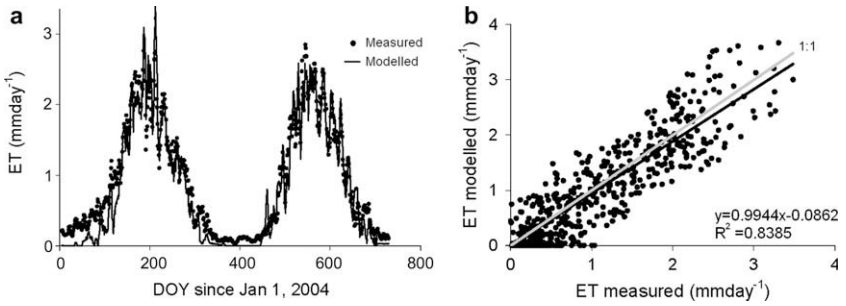

Fig. 7. (a) Comparison of simulated and measured ET time-series (5-day moving average) for the years 2004 and 2005, at the EOBS-tower footprint region. (b) One-to-one comparison of simulated and measured ET for the years 2004 and 2005 (combined).

sensed by the EC tower, which the model has underestimated. Analysis of meteorological data revealed that the winter of 2004 was much colder and drier than 2005 and this might have resulted in increased sublimation of snow pack in 2004. There are studies that demonstrate that sublimation of intercepted snow constitutes a significant component of the water balance of boreal ecosystems (Lundberg and Halldin, 1994). Based on EC measurements, Molotch et al. (2007) suggests that the intercepted snowfall results in rapid response of above-canopy latent heat fluxes as high as 3.7 mm day^{-1}. Another factor that might explain the discrepancies between the simulated and measured ET could be the presence of Lake Inlet situated about 900 m northwest of the EOBS tower. It is speculated that "lake effect" could slightly influence latent heat flux measurements because advective process could alter the local humidity, altering the vapor pressure deficit at the tower site, depending on wind patterns. However, in general, the lake was not in the sector of the EOBS-tower footprint. But on some windy days, this effect cannot be completely ruled out.

The annual total ET loss at the FCRN tower site was simulated to be 330.2 mm (325 mm measured) and 257.67 mm (287 mm measured), in 2004 and 2005, respectively. Fig. 8a and b show the spatial distributions of annual ET simulated for the 2 years. The spatial distribution of the simulated annual ET reflects the combined effects of physiological variations in plant functional types, topographical and soil textural controls on soil moisture and the influence of canopy architectural features on canopy radiative transfer mechanisms. On this boreal landscape, simulated values of annual ET are highly controlled by vegetation-type having unique ecophysiological attributes. Topography was identified as a major control governing the distribution of plant functional types. Coniferous stands have an annual average (spatial average of the annual values) simulated ET of 307 mm (2004) and 302 mm (2005). Mixed forest stands have an annual average ET of 441 mm (2004) and 441.5 mm (2005). Wetlands, on the other hand, have an annual average ET of 267 mm (2004) and 278 mm (2005).

In this humid boreal ecosystem, water is not a scarce resource for plant functioning. Factors that govern the level of resistance imparted by a vegetated land surface on the potential rate of ET were: vegetation type, presence of moss layer on the forest-floor, soil texture and meteorological factors. Even under conditions of unlimited water supply, ET may not proceed at rates determined by the available energy and vapor pressure deficits (Roberts, 2007) because ET is highly influenced by transpiration, which is strongly controlled by vegetation characteristics such as LAI, vegetation height, maximum stomatal conductance ($g_{s,max}$), and the nature of canopy architectures that control radiative transfer. Since deciduous and mixed stands have higher $g_{s,max}$ than conifers (see Table 1 and Appendix A), the ambient g_s values in the former are relatively higher than the latter which results in greater amount of transpirational losses in deciduous stands than evaporational losses. At lower elevations of the watershed where the WTDs are shallower, plants are subjected to stress as a result of saturated soil conditions resulting in lower ET. In a measurement study conducted in a boreal forest in Saskatchewan in central Canada (Amiro et al., 2006), it

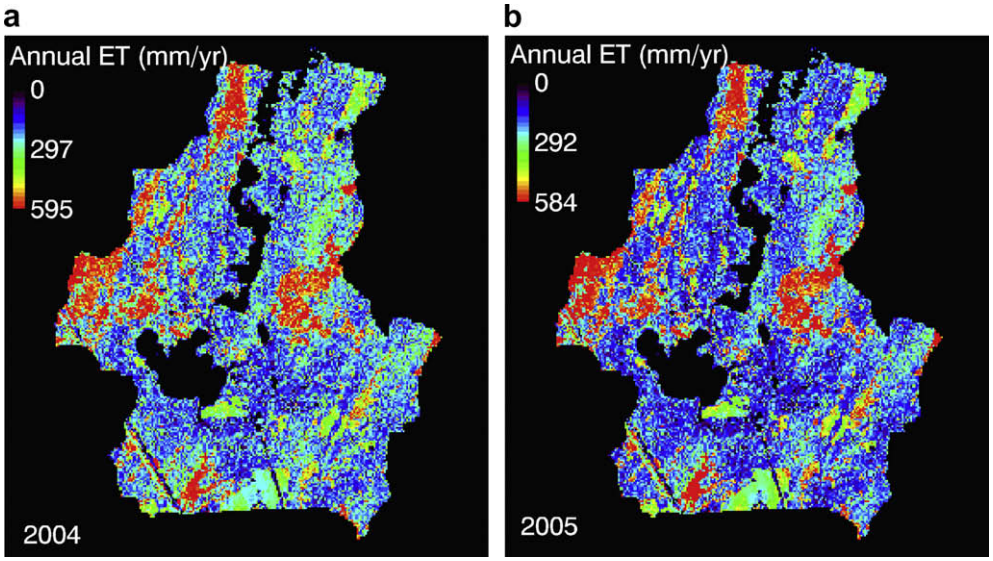

Fig. 8. Spatial distributions of annual total ET simulated by BEPS-Terrainlab for (a) 2004 and (b) 2005 for the watershed surrounding the EOBS flux tower. The scale of the ~40 km^2 watershed is shown in Fig. 2.

was shown that lower elevation regions in spite of having shallower WTD, did not show higher values of ET.

Watershed-scale ET is the combination of several sub-component processes that are both physical (e.g. evaporation of intercepted water on canopy, sublimation and soil evaporation) and biological (e.g. transpiration) in nature, all of which occur simultaneously. The magnitudes of ET sub-components reflect the characteristic feature of a land-cover. For example, in black spruce stands where the overstory canopy is generally open (Heijmans et al., 2004), the forest-floor evaporation is a significant contributor to the total ET because of relatively lower transpiration from overstory and understory canopies. Since it is assumed that a moss layer covers 85% of a black spruce forest-floor, only 15% is exposed soil surface (see Table 1). Therefore, the major contributor of forest-floor evaporation in black spruce stands is moss evaporation, rather than soil evaporation. Deciduous and mixed forests have relatively higher contributions from overstory and understory transpiration rather than forest-floor evaporation. The novel contribution of BEPS-Terrainlab V2.0 lies in explicitly modeling transpiration, evaporation and sublimation using surface-specific (canopy, moss or soil) radiation and resistance terms that contributes to the total ecosystem ET. This method of ET calculation is critical for hydro-ecological representations in boreal ecosystems because ET is a significant component of the soil water balance.

Volumetric soil water content (VSWC) and water-table depth (WTD)

Fig. 9 shows the temporal dynamics of the modeled VSWC at the location where VSMC measurements are being made using a TDR (average of 0–50 cm) in the EOBS tower-footprint region. The VSWC varied quite rapidly during the course of the year in response to precipitation and other hydrological processes. The model was able to capture the temporal pattern in fair agreement with the measurements for most parts of the growing season. The model adequately captured the steep decline in VSWC between DOY 200–230 in 2004 and DOY 200–250 in 2005. It can be concluded that VSWC remains near field capacity during the late spring and rarely falls below the permanent wilting point even in mid-summer.

Discrepancies arise because in BEPS-TerrainLab V2.0, VSWC is the average of the entire unsaturated zone. This discrepancy could be reduced only if multi-layer unsaturated zone moisture movement is incorporated by numerically solving the Richards equation with space, time and depth varying soil hydraulic properties. Scale inconsistencies that underlie this comparison also need to be considered. Here, a point-scale measurement of VSWC is compared with a simulation estimate for a 25 m^2 pixel, which makes a quantitative comparison very difficult. Future improvements in BEPS-Terrainlab V2.0 could incorporate multi-layered vadose zone processes in a spatially explicit manner.

To test the performance of the model for WTD simulation, the measurements taken by a Solinst level-logger were compared to the simulated WTD (Fig. 10). Measurements taken at two-hour intervals were converted to daily mean values for comparison. The model was able to explain 69% and 76% of the measured variability between the days 120 and 365 for 2004 and 2005, respectively. The comparison showed that the model performance was satisfactory during much of the growing season, autumn and early winter, and captured the overall WTD trend in both the years. During the mid-growing season in 2004, between the days 200–240 and 241–271, the WTD declined rapidly due to prolonged dry periods in combination with optimum conditions for ET losses. Similarly in 2005 as well, there was a prolonged dry period between the days 180 to 270. The model captured this rapid decline as well as the subsequent rise of WTD. The model was able to simulate the dynamics of WTD because various components of the water balance were modeled with reasonable accuracy.

In 2004, on DOY 247, an intense single day precipitation event made the WTD rise rapidly within a few hours (as inferred from the two-hourly measurement data). Although the model captured this dynamics, the simulated magnitude did not agree fully with the measurements. This can be speculated as a scale related issue because a net SOLF was simulated in the tower footprint as a whole on DOY 247. In BEPS-TerrainLab V2.0, SOLF occur only when the soil profile is saturated, i.e., when WTD $\leqslant 0$. This implies that in the modeling domain there was a rapid rise (getting near to surface) of WTD which triggered SOLF.

Another discrepancy was seen in the early spring when the model generally underestimated the simulated WTD. This is probably due to a weaker parameterization of the snowmelt process wherein the contribution of snowmelt in raising the WTD appears to be underestimated. Since a quasi-physical snowmelt model was adopted, it is probable that a higher accuracy in the snowmelt process was not achieved. Again, scale issues must be considered while analyzing various discrepancies between the measured and modeled WTDs. Point–scale measurements were compared with the simulated dynamics of the WTD in a pixel that has an area of 625 m^2.

Sub-surface baseflow, surface over-land flow and the water balance

The tower-footprint average lateral sub-surface baseflow is shown in Figs. 11a and b for 2004 and 2005, respectively. The baseflow flux is calculated using a modified approach that accommodates the preferential water fluxes through the moss–peat layer. The patterns of the baseflow time-series resemble the seasonal fluctuations in WTD because the previous day WTD is used to calculate baseflow fluxes. The simulated baseflow time-series looks reasonable because most of the seasonal patterns were captured (i.e., spring season peak discharge and the mid-summer recession).

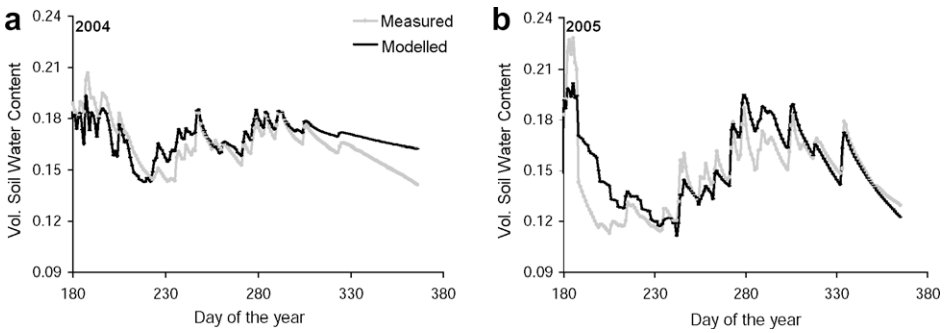

Fig. 9. Simulated vs. modeled VSWC at the EOBS flux tower footprint for the years (a) 2004 and (b) 2005.

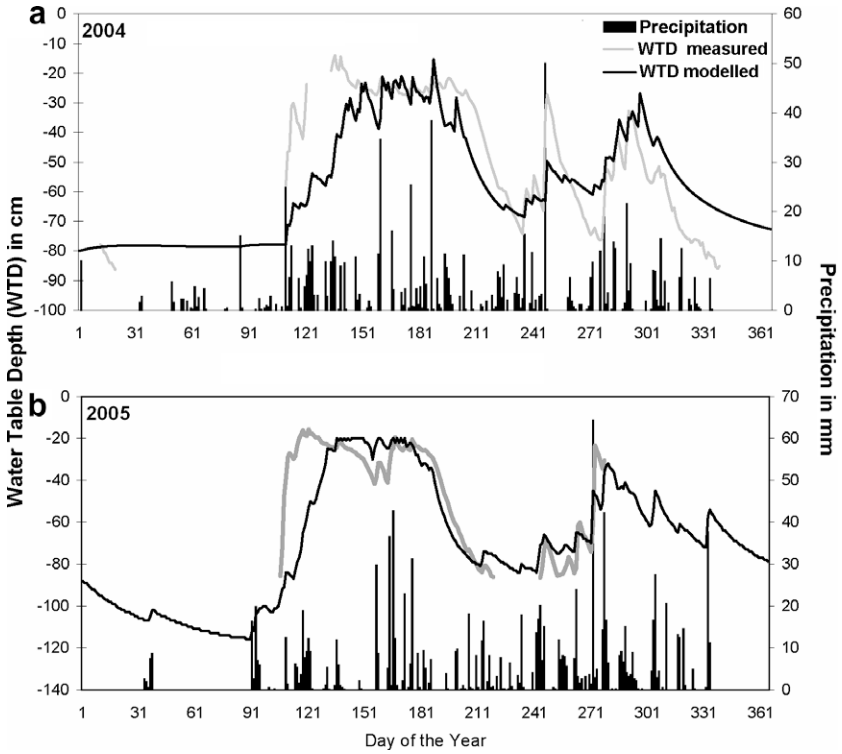

Fig. 10. Comparison of simulated and measured WTD fluctuations at the EOBS flux tower site for the years (a) 2004 and (b) 2005.

In the spring, there was an upsurge in baseflow flux due to the rapid saturation of the soil profile with snowmelt water. Since the process of snowmelt affects the WTD, soil transmissivity increases correspondingly, leading to large baseflow fluxes. Our simulations show that annually, around 637 mm and 552 mm of water was lost from the footprint region through baseflow fluxes, which were 64% and 66% of the annual infiltrated water (through-fall + stemflow + snowmelt), in 2004 and 2005, respectively. Responses of baseflow fluxes toward precipitation events were different for different soil types due to differences in their inherent hydraulic properties. Since there was no runoff measurement at the EOBS site, validation of the baseflow fluxes were not possible.

The simulated annual footprint average SOLF was 79.4 mm and 69.1 mm in 2004 and 2005, respectively. Most of the SOLF occurred between the days 134 and 195 in 2004 coinciding with the snowmelt period. On the day 247 in 2004, a high intensity precipitation

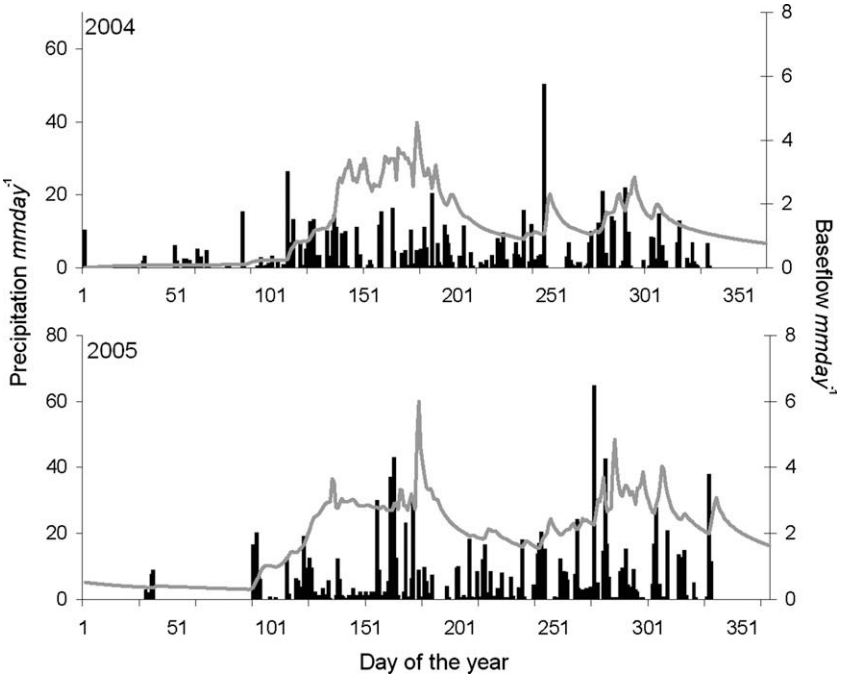

Fig. 11. Simulated baseflow fluxes for the years 2004 and 2005 at the EOBS-tower-footprint area.

event occurred that lasted only a few hours when SOLF was the main mechanism of water loss. Similarly, in 2005, SOLF mostly occurred during the days before and after the mid-growing season when high intensity precipitation events occurred. A comparison of the magnitudes of SOLF and sub-surface baseflow reveals that the latter is the most dominant process that partitions soil water in this humid boreal ecosystem. The presence of macroporous conduits in the moss-peat layer creates preferential pathways for the water to move across the terrain making sub-surface baseflow a dominant lateral water flow mechanism in this ecosystem.

It is probable that the sub-surface geology of the landscape has a critical role in governing the lateral movement of sub-surface water. In the Canadian Shield, where the study site is located, shallow soils underlain by impermeable crystalline bedrock represents the dominant sub-surface geology and thus, the confining layer often mimics the surface topography (Price et al., 2005). In this situation, WTD dynamics is a direct function of localized recharge, sub-surface fluxes and ET losses resulting in relatively simpler WTD dynamics as a function of shorter term variation in weather (precipitation and ET). Thus, the dynamics of WTD and flow rates in these types of boreal settings is simply a reflection of bedrock geomorphology consequent of shallow soils.

An annual water balance in the footprint region reveals the following information. The total annual precipitation was 1,053 mm and 902 mm in 2004 and 2005, respectively. Of this precipitation, 63.7 mm (2004) and 65.2 mm (2005) were intercepted on the vegetation canopy and some portion of the intercepted precipitation, i.e., 58.2 mm (2004) 40.7 mm (2005) were evaporated directly to the atmosphere. The remaining 5.5 mm (2004) and 24.5 mm (2005) reached the ground as stem-flow and drips. In 2004, since the precipitation was comparatively of lower intensity and evenly distributed, the stem-flow was much lower and most of the canopy intercepted water directly evaporated or sublimed. Through-fall, which directly reached the ground through canopy gaps, was 732.6 mm (2004) and 661.3 mm (2005). Snowmelt accounted as much as 256.0 mm in 2004 and 175.7 mm in 2005. The infiltrated water that entered the soil profile consisted of through-fall, stem-flow and snowmelt constituted 989.0 mm and 837.0 mm of water in 2004 and 2005, respectively.

The footprint average annual soil water balance shown in Fig. 12 describes how the soil hydrological processes were partitioned annually. Inputs include the infiltrated water (sum of through-fall, stem-flow and snowmelt), inflowing SOLF and inflowing sub-surface baseflow. The outputs include ET (all sub-components except canopy evaporation or sublimation), outflowing SOLF and outflowing sub-surface baseflow. The storage change of moisture in the soil profile of the tower footprint equals the difference between the inputs and outputs as shown in Eq. (9).

The bottom-line of this analysis reveals that the most dominant form of soil water partitioning in this ecosystem is sub-surface baseflow, which is approximately 65% of the annual infiltrated water into the soil. This is followed by ET losses, which is around

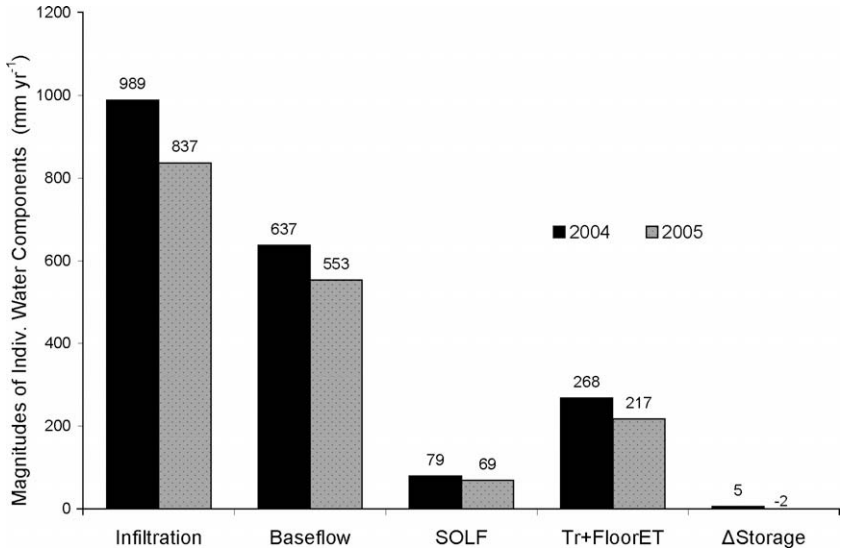

Fig. 12. Simulated magnitudes of soil water balance components in the EOBS footprint region in 2004 and 2005, between days 1 and 365.

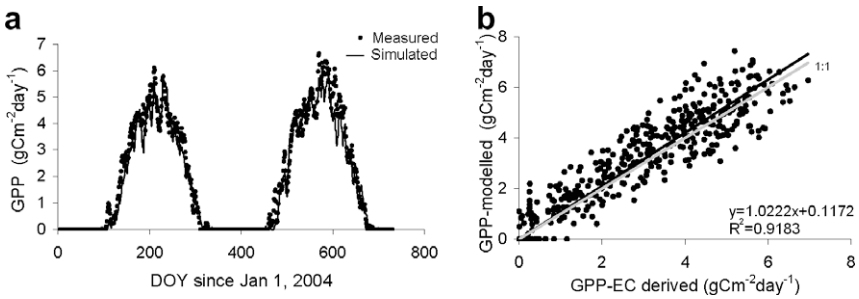

Fig. 13. (a) Comparison of simulated and measured GPP time-series (5-day moving average) for the years 2004 and 2005, at the EOBS-tower-footprint area. (b) One-to-one comparison of simulated and measured GPP for the years 2004 and 2005 (combined).

26% of the annual infiltrated water. SOLF was not a dominant mechanism of lateral soil water delivery in humid boreal settings.

Spatiotemporal patterns of GPP

Having gained a detailed understanding of the hydrological processes in this humid boreal ecosystem, hydrologically controlled carbon dynamics was further explored. Fig. 13 shows the comparison of the tower-footprint average simulated daily GPP and EC-derived GPP for 2004 and 2005. The model explained 91% and 92% of the variability in measured GPP, in 2004 (RMSE = 0.42 gC m^{-2} yr^{-1}) and 2005 (RMSE = 0.51 gC m^{-2} yr^{-1}), respectively. The main discrepancies were observed during the peak growing periods when the model was highly sensitive to soil water status. During the model development phase, an overestimation of the simulated GPP in spring was a problem. It was found that this overestimation was due to an unrealistic representation of the plant physiological status when the ambient air temperature was used for the calculation of g_s, which affected the simulated photosynthesis. In reality, during the spring, soil temperature remains much lower which keeps the vegetation in a physiologically inactive state. This problem was rectified by introducing two major modifications to the model: (1) a soil temperature scalar was introduced into the Jarvis algorithm (Eq. (A1) in the Appendix A) which improved the simulation of g_s and (2) a soil nitrogen cycle was introduced in conjunction with the soil C-cycle which facilitated the realistic N-mineralization in the soil (Govind et al., in press).

For each land-cover type, there were unique GPP sub-component contributions (i.e., overstory, understory and moss) to the total GPP. The magnitudes of these fractions greatly depend on various factors such as g_s, soil moisture, soil temperature and soil N dynamics, which directly or indirectly depend on the local hydrological processes. Our approach of modeling the total ecosystem GPP as the sum of overstory, understory and moss components and employing a quasi-physiological spatial upscaling strategy is a novel method of quantifying ecohydrological processes (see Appendix A for model details). The simulated annual average GPP in the footprint region is 613 gC m^{-2} yr^{-1} (592 gC m^{-2} yr^{-1} measured by the EC technique) and 709 gC m^{-2} yr^{-1} (680 gC m^{-2} yr^{-1} measured by the EC technique), in 2004 and 2005, respectively.

The spatial distribution of the simulated annual GPP (Fig. 14) reveals that deciduous and mixed forests have high annual photosynthesis (annual averages of 1,046 and 1,250 gC m^{-2} yr^{-1}in 2004 and 2005, respectively) as opposed to conifer stands (annual averages of 610 and 704 gC m^{-2} yr^{-1}in 2004 and 2005, respectively) or wetlands (annual average of 457 and 501 gC m^{-2} yr^{-1} in 2004 and 2005, respectively). Deciduous stands have higher stomatal conductance ($g_{s,max}$ = 5 mm s^{-1}) as opposed to conifer stands ($g_{s,max}$ = 1.6 mm s^{-1}). Moreover, leaves in deciduous canopies are less clumped (Ω = 0.8–0.9) than in conifers (Ω = 0.5–0.6), and this increases the probability of sunlit leaves in a deciduous canopy than shaded leaves.

Summary and conclusions

A process-based, spatially distributed, hydro-ecological model, BEPS-TerrainLab V2.0 was further developed to understand the strong links between hydrological, ecophysiological and biogeochemical processes unique to boreal ecosystems. Novel contributions of this study include explicit ecophysiological modeling of multi-layered and multi-stressed vegetation canopies and development of conceptualizations that are unique to humid boreal ecosystems. This model can thus be used as a learning tool to understand the hydro-ecological feedbacks in boreal ecosystems in a spatially explicit manner.

The model was evaluated using various types of measurements taken for 2 years. Comparison of the simulations with the measurements reveals that BEPS-TerrainLab V2.0 can adequately simulate various hydro-ecological processes such as ET, dynamics of WTD, VSMC and photosynthesis. From the lessons learned during model development and from the model testing phases, the following conclusions can be drawn:

1. Since boreal forest-floors are predominantly covered by a moss-peat layer, lateral water fluxes take preferential pathways through this highly permeable layer. Based on laboratory measurements, preferential flow of water was conceptualized and quantified which substantially improved hydrological simulations in boreal settings. More laboratory experiments on peat hydraulic properties and peat-specific pedo-transfer functions are required for an improved understanding of hydrological processes in boreal ecosystems.
2. Simultaneous consideration of the fractions of LAI that corresponds to different moisture and light regimes can be effectively used as weighting factors to upscale leaf-level ecophysiological processes such as transpiration and photosynthesis. This strategy allows efficient upscaling of plant physiological processes by mimicking the environmental stress factors affecting the ecophysiological processes (see Appendix A).

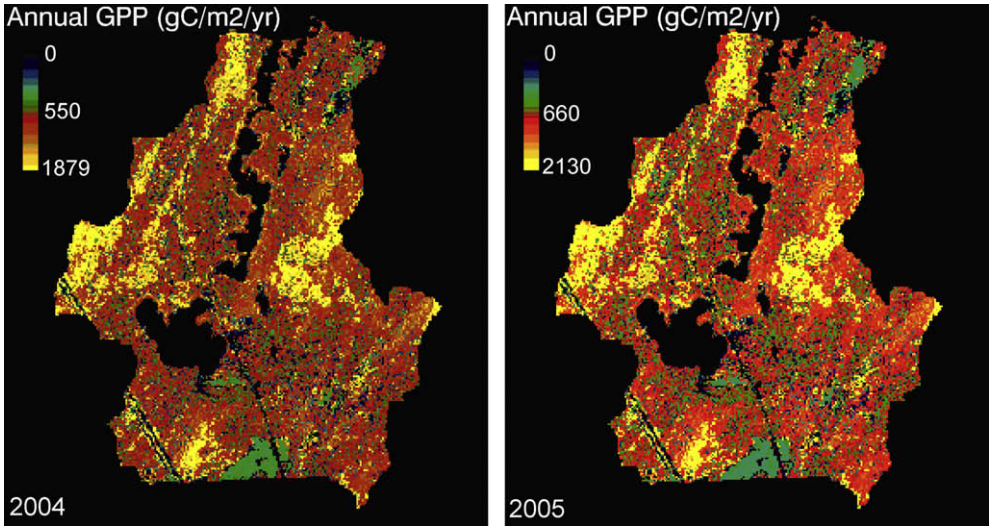

Fig. 14. Spatial distribution of GPP simulated for the years 2004 and 2005. The scale of the ~40 km^2 watershed is shown in Fig. 2.

3. In humid eastern North American boreal ecosystems, subsurface baseflow is the main mechanism of groundwater redistribution, which is almost 63–65% of the infiltrated water. Hence, proper accounting of this process is critical to improve our understanding of hydro-ecological connectivity.

Although it is intuitive that landscape-scale hydrological processes affect local-scale water balance and biogeochemical processes, many large-scale ecological models ignore explicit hydrological controls. To test this hypothesis and to better understand the errors inherently present in the simulated ecological and biogeochemical processes, it is imperative to have models that have strong coupling between various processes in the soil-plant-atmospheric continuum in a spatially explicit manner similar to BEPS-Terrainlab V2.0. This is likely to decipher hydro-ecological interactions and nonlinear feedback relations to make us better understand the terrestrial C-cycling process under changing climate. Considering the fact that many of the large-scale C-cycling models ignore hydrological controls, the current understanding of the spatio-temporal distribution of terrestrial C-sources and sinks is speculative because of the large topographic variations on the earth's surface that significantly affect local-scale hydrology.

Acknowledgements

This work was supported by the Canadian Carbon Program (formerly, Fluxnet-Canada Research Network), funded by the Canadian Foundation for Climate and Atmospheric Sciences (CFCAS), Natural Sciences and Engineering Research Council of Canada (NSERC) and BIOCAP Canada. We thank Pierre Bernier of the Laurentian Forestry Centre, Canadian Forest Service, Quebec, Canada, for providing various datasets (soil texture, gas exchange measurements) originating from the ECOLEAP project. Jeff McDonnell at the Oregon State University is acknowledged for fruitful discussions regarding the preferential water fluxes while AG visited his lab in 2006. We thank André Beaudoin and Luc Guindon of the Laurentian Forestry Centre, Canadian Forest Service, Quebec, Canada, for providing the land-cover map originating from the Earth Observation for Sustainable Development of Forests (EOSD) project. We also thank Onil Bergeron and Carole Coursolle, Université Laval, Quebec, Canada, for their efforts in processing the flux and meteorological measurements at EOBS. The authors acknowledge Mircea Pilaf, engineering technologist, University of Toronto, for his assistance with the constant head permeameter for measuring $K_{sat,peat}$.

Appendix A. Hydro-ecological processes considered in BEPS-TerrainLab V2.0

Stomatal. conductance, moss conductance and soil conductance

Stomatal dynamics play a key role in most the ecophysiological processes because it is one of the primary links in the soil-plant-atmosphere continuum of mass and energy. In BEPS-TerrainLab V2.0, the multiplicative approach proposed by Jarvis (1976) is used to constrain a maximum stomatal conductance ($g_{s,\max}$), for water vapor transport. In this approach various scalars that represent environmental factors constrain a species-specific $g_{s,\max}$ (see Table 1) to return the ambient g_s.

Although more sophisticated models of stomatal dynamics are available in the literature (e.g. Ball et al., 1987 or Leuning, 1997), we chose to adopt the Jarvis approach because in a distributed modeling scenario, employing a mechanistic stomatal conductance model is computationally challenging. A mechanistic g_s model requires iterative calculations in order to update the ambient g_s for CO_2 by equilibrating it with photosynthesis at a previous time-step. We believe that the Jarvis algorithm is best suited for spatially explicit hydro-ecological modeling considering our current computational constraints. We made a further modification to the Jarvis method by including a new scalar that represents the effect of yet another environmental factor, i.e. soil temperature following Heddeland and Lettenmaier (1995). This modification is important because in boreal regions, during spring, soil temperature remains much lower than air temperature. This condition makes the plant physiologically inactive and limits water uptake and growth (Bonan and Shugart, 1989). The modified Jarvis algorithm after the inclusion of a scalar for soil temperature ($f_5(T_s)$) can be summarized as shown below:

$$g_s = g_{s\max} \cdot \lfloor f_1(F_p) \times f_2(T_a) \times f_3(D_v) \times f_4(\theta_{sw}) \times f_5(T_s) \rfloor \quad \text{(A1)}$$

In Eq. (A1), $g_{s,\max}$ is a land-cover specific maximum stomatal conductance (see Table 1). F_p is the photosynthetic photon flux density (PPFD), T_a is the mean air temperature, D_v is vapor pressure deficit and θ_{sw} = VSMC for the unsaturated moisture regime or $\theta_{sw} = \varphi$ for the saturated moisture regime (assumed as porosity), depending on the physiological statuses of leaves (described in the 'Spatial upscaling of transpiration and photosynthesis'). The functions, f_{1-4} for calculating these scalars can be found in Chen et al. (2005). The new scalar $f_5(T_s)$ is calculated as shown in Fig. A1a. Soil temperature, T_s, is calculated by numerically solving the Fourier heat transfer equation for a 5-layered soil profile (Govind et al., in press).

Finally, the total conductance ($g_{s,total}$) is calculated by considering the cuticular conductance ($g_{cuticle}$) and g_s in parallel and boundary layer conductance ($g_{boundary}$) in series. Such that the total stomatal conductance for water vapor exchange becomes:

$$g_{s,t} = \frac{g_{boundary} \times (g_{cuticle} + g_s)}{g_{boundary} + g_{cuticle} + g_s} \quad \text{(A2)}$$

The reciprocal of $g_{s,t}$, i.e., stomatal resistance calculated in this manner (m s^{-1}) is directly used in Eq. (1) for ET calculations. For photosynthesis, $g_{s,t}$ is reduced by a factor of 0.625 to account for CO_2 exchange. Fig. A1 shows a qualitative comparison of the simulated g_s (average for all leaf types) with the measurements (Bernier et al., 2005) taken at the footprint region using an ADC LC-Pro photosynthesis system in the growing season of 2004. For the moss layer, the conductance is calculated using a least squares regression after Williams and Flanagan (1998) and for the conductance of soil surface, it is calculated directly as a function of VSMC.

Leaf. fractions in a canopy corresponding to varying light and water regimes

To quantify the fraction of leaves in a given light regime, we adopted the conceptualization outlined by Chen et al. (1999) where the total LAI is partitioned based on canopy radiative transfer mechanism as shown below.

$$\text{LAI}_{over} = \text{Total Leaf Area Index of the canopy}$$

$$\text{LAI}_{over,sun} = 2 \cdot Cos\theta \cdot \left(1 - \exp\left[-\frac{0.5 \cdot \Omega \cdot \text{LAI}}{Cos\theta}\right]\right) \quad \text{(A3)}$$

where $\text{LAI}_{over,sun}$ is the sunlit LAI of overstory, θ = Solar Zenith Angle, Ω is the Canopy Clumping Index.

$$\text{LAI}_{over,shade} = \text{LAI}_{over} - \text{LAI}_{over,sun} \quad \text{(A4)}$$

$\text{LAI}_{over,shade}$ is the shaded LAI of overstory.

LAIs in the understory canopy and for the forest-floor are not fractionated into components in various light regimes because the nature of radiative transfer is complicated within the understory and on the forest-floor.

In order to quantify the fractions of leaves in a canopy that correspond to different soil moisture regimes, we employ the Pipe

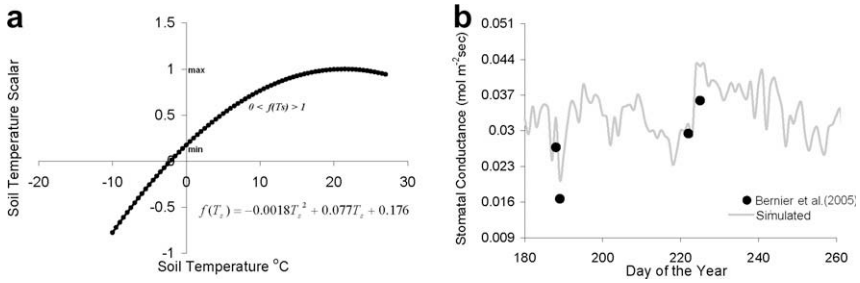

Fig. A1. (a) The soil temperature scalar $f(T_s)$ used to constrain g_{max} for a wide range of soil temperature values. (b) Footprint average (all leaf types) simulated g_s in comparison to measurements taken using an ADC LC-Pro-photosynthesis system in the growing season of 2005.

Theory (Shinozaki et al., 1964a and Shinozaki et al., 1964b) and assume that the shoots and roots are proportional with respect to moisture regimes. With this simplification, fractions of roots lying in the saturated and unsaturated zones are directly used in an upscaling strategy (Eqs. (A6) and (A8)). We use a simple root extinction coefficient χ to determine the proportion of roots that are lying in the saturated and the unsaturated zones. Depending on the position of the WTD and root geometry, these fractions are calculated following a simple empirical approach suggested by Gale and Grigal (1987).

$$f(\mu) = \mu_j = 1 - \chi^{z_j} \tag{A5}$$

where μ_j is the root fraction in the unsaturated zone, and χ is the root extinction coefficient, which is a species-specific value and z_i is the WTD (in cm). A high value of χ (e.g., 0.98) indicates a deep root system. A typical χ value for the boreal forest is ~0.943 (Jackson et al., 1996). For the present study, the understory root distribution coefficient χ_{under} was assumed to be 75% of the overstory value, implicitly describing the understory as shallow rooted plants. Refer to Table 1 for species-specific root extinction coefficients, typical of a boreal ecosystem.

Spatial. upscaling of transpiration and photosynthesis

Conceptualizations of transpiration and photosynthesis using the Penman–Monteith and the Farquhar models, respectively, are applicable at the leaf scale. In order to upscale these processes to the canopy scales, spatial upscaling strategies are required. In BEPS-TerrainLab V2.0, it is assumed that light and soil moisture are the governing factors that distinguish physiological statuses of the leaves within a canopy. Light and moisture variations result in unique leaf-level physiological differences which manifest into variations in g_s. Leaf-level processes are spatially upscaled using weighting fractions of LAI (as shown above) that correspond to a given light (sunlit or shaded) and soil moisture regime (saturated or unsaturated). Unlike the previous versions of the model that used a *big-leaf* (e.g. TerrainLab, Chen et al., 2005) or *sunlit-shaded* approaches (BEPS, Liu et al.,1997 and Liu et al.,2003) to calculate the ecosystem scale ET and photosynthesis, respectively, BEPS-TerrainLab V2.0 employs a modified sunlit-shaded leaf strategy and it is called as a *four-leaf approach* because it is assumed that within each light regime, there are two states of moisture regimes. Leaf-level transpiration or photosysnthesis calculated using unique g_s is upscaled to canopy-scale by weighting with their respective LAI fractions. Such that:

$$\begin{aligned} T_o = {} & \lfloor T_{sun,unsat} \cdot \mathrm{LAI}_{over,sun} \cdot \mu + T_{sun,sat} \cdot \mathrm{LAI}_{over,sun}(1-\mu) \rfloor \\ & + [T_{shade,unsat} \cdot \mathrm{LAI}_{over,shade} \cdot \mu + T_{shade,sat} \cdot \mathrm{LAI}_{over,shade}(1-\mu)] \end{aligned} \tag{A6}$$

$$\begin{aligned} T_{sun,sat} &= f_1(R_{n\,sun} g_{s,sun,sat}, \phi) \\ T_{sun,unsat} &= f_1(R_{n\,sun} g_{s,sun,sat}, \theta) \\ T_{shade,sat} &= f_1(R_{n\,shade} g_{s,shade,sat}, \phi) \\ T_{shade,unsat} &= f_1(R_{n\,shade} g_{s,shade,unsat}, \theta) \end{aligned} \tag{A7}$$

where, T_o is the overstory canopy transpiration and the function f_1 is Penman–Monteith equation, which uses unique surface-specific net radiations (R_n) and g_s. Here μ is fraction of roots in the unsaturated zone and $(1-\mu)$ is the fraction of roots in saturated zone that proportionately corresponds to physiological status of the leaves in the canopy, as described in the previous section.

Similarly, photosynthesis is spatially upscaled using LAI fractions that correspond to different leaf physiological statuses in a manner similar to the spatial upscaling strategy adopted for transpiration (*four-leaf approach*) for overstory canopy.

$$\begin{aligned} A = {} & \lfloor A_{sun,unsat} \cdot \mathrm{LAI}_{sun} \cdot \mu + A_{sun,sat} \cdot \mathrm{LAI}_{sun}(1-\mu) \rfloor + [A_{shade,unsat} \\ & \cdot \mathrm{LAI}_{shade} \cdot \mu + A_{shade,sat} \cdot \mathrm{LAI}_{shade}(1-\mu)] \end{aligned} \tag{A8}$$

$$\begin{aligned} A_{sun,sat} &= f_2(R_{s,sun}, g_{s,sun,sat}, \phi) \\ A_{sun,unsat} &= f_2(R_{s,sun}, g_{s,sun,sat}, \theta) \\ A_{shade,sat} &= f_2(R_{s,shade}, g_{s,shade,sat}, \phi) \\ A_{shade,unsat} &= f_2(R_{s,shade}, g_{s,shade,unsat}, \theta) \end{aligned} \tag{A9}$$

A in Eq. (A8) is the overstory canopy's photosynthesis which has sub-components that are calculated explicitly for combinations of radiation (R_s) and moisture regimes based on the function, f_2, which is the temporally integrated Farquhar model of Chen et al. (1999).

For the understory canopy,however, a *quasi-big-leaf approach* is employed as the upscaling strategy using a canopy conductance $g_{c,under}$, which is simply calculated as $g_{sunder} \times \mathrm{LAI}_{under}$ for both transpiration and photosynthesis. However, the relative understory contribution from the saturated and unsaturated zones is considered in BEPS-TerrainLab V2.0. The understory transpiration and photosynthesis can be expressed as given below:

$$T_{under} = (T_{under} \cdot \mu_{under}) + (T_{under} \cdot (1-\mu_{under})) \tag{A10}$$

$$A_{under} = (A_{under} \cdot \mu_{under}) + (A_{under} \cdot (1-\mu_{under})) \tag{A11}$$

This is a novel way of explicitly describing plant physiological statuses within a canopy. Future research works can improve this scheme to better represent multiple plant stress factors in addition to light and water.

Appendix B. Supplementary data

Supplementary data associated with this article can be found, in the online version, at doi:10.1016/j.jhydrol.2009.01.006.

References

Amiro, B.D., Davis, P.A., 1988. Statistics of atmospheric-turbulence within a natural black spruce forest canopy. Boundary-Layer Meteorology 44, 267–283.

Amiro, B.D., Barr, A.G., Black, T.A., Iwashita, H., Kljun, N., Mccaughey, J.H., Morgenstern, K., Murayama, S., Nesic, Z., Orchansky, A.L., Saigusa, N., 2006. Carbon, energy and water fluxes at mature and disturbed forest sites, Saskatchewan, Canada. Agricultural and Forest Meteorology 136, 237–251.

Baldocchi, D., Valentini, R., Running, S., Oechel, W., Dahlman, R., 1996. Strategies for measuring and modelling carbon dioxide and water vapour fluxes over terrestrial ecosystems. Global Change Biology 2, 159–168.

Ball, J.T., Woodrow, I.E., Berry, J.A., 1987. A model predicting stomatal conductance and its contribution to the control of photosynthesis under different environmental conditions. In: Progress in Photosynthesis Research. Martinus Nijhoff Publishers, Dordrecht, pp. 221–224.

Band, L.E., Patterson, P., Nemani, R., Running, S.W., 1993. Forest ecosystem processes at the watershed scale – incorporating hillslope hydrology. Agricultural and Forest Meteorology 63, 93–126.

Band, L.E., Tague, C.L., Groffman, P., Belt, K., 2001. Forest ecosystem processes at the watershed scale: hydrological and ecological controls of nitrogen export. Hydrological Processes 15, 2013–2028.

Beckers, J., Alila, Y., 2004. A model of rapid preferential hillslope runoff contributions to peak flow generation in a temperate rain forest watershed. Water Resources Research 40.

Bergeron, O., Margolis, H.A., Black, T.A., Coursolle, C., Dunn, A.L., Barr, A.G., Wofsy, S.C., 2007. Comparison of carbon dioxide fluxes over three boreal black spruce forests in Canada. Global Change Biology 13, 89–107.

Beringer, J., Lynch, A.H., Chapin, F.S., Mack, M., Bonan, G.B., 2001. The representation of arctic soils in the land surface model: the importance of mosses. Journal of Climate 14, 3324–3335.

Bernier, P.Y., Boivin-Chabot, S., Dagnault, S., 2005. Gas exchange in black spruce at Fluxnet mature site, Chibougamau, Québec, Canada. ECOLEAP Project, Canadian Forest Service, Natural Resources Canada.

Betts, R.A., Boucher, O., Collins, M., Cox, P.M., Falloon, P.D., Gedney, N., Hemming, D.L., Huntingford, C., Jones, C.D., Sexton, D.M.H., Webb, M.J., 2007. Projected increase in continental runoff due to plant responses to increasing carbon dioxide. Nature 448, 1037–1041. doi:10.1038/nature06045.

Beven, K.J., Kirkby, M.J., 1979. A physically based variable contributing model of basin hydrology. Hydrological Science Bulletin 24, 43–69.

Blodau, C., Roulet, N.T., Heitmann, T., Stewart, H., Beer, J., Lafleur, P., Moore, T.R., 2007. Belowground carbon turnover in a temperate ombrotrophic bog. Global Biogeochemical Cycles 21.

Bonan, G.B., 1995. Land atmosphere CO_2 exchange simulated by a land-surface process model coupled to an atmospheric general-circulation model. Journal of Geophysical Research – Atmospheres 100, 2817–2831.

Bonan, G.B., Shugart, H.H., 1989. Environmental-factors and ecological processes in boreal forests. Annual Review of Ecology and Systematics 20, 1–28.

Campbell, G.S., Norman, J.M., 1998. An Introduction to Environmental Biophysics. Springer-Verlag, New York. pp. 1291–144.

Chen, J.M., Liu, J., Cihlar, J., Goulden, M.L., 1999. Daily canopy photosynthesis model through temporal and spatial scaling for remote sensing applications. Ecological Modelling 124, 99–119.

Chen, J.M., Ju, W.M., Cihlar, J., Price, D., Liu, J., Chen, W.J., Pan, J.J., Black, A., Barr, A., 2003. Spatial distribution of carbon sources and sinks in Canada's forests. Tellus Series B – Chemical and Physical Meteorology 55, 622–641.

Chen, J.M., Chen, X.Y., Ju, W.M., Geng, X.Y., 2005. Distributed hydrological model for mapping evapotranspiration using remote sensing inputs. Journal of Hydrology 305, 15–39.

Chen, J.M., Govind, A., Sonnentag, O., Zhang, Y.Q., Barr, A., Amiro, B., 2006. Leaf area index measurements at Fluxnet-Canada forest sites. Agricultural and Forest Meteorology 140, 257–268.

Chen, X.F., Chen, J.M., An, S.Q., Ju, W.M., 2007. Effects of topography on simulated net primary productivity at landscape scale: carbon sequestration in China's forest ecosystems. Journal of Environmental Management 85, 585–596.

Cionco, R.M., 1978. Analysis of canopy index values for different canopy densities. Bulletin of the American Meteorological Society 59, 1507.

Coops, N.C., Black, T.A., Jassal, R.P.S., Trofymow, J.A.T., Morgenstern, K., 2007. Comparison of modis, Eddy covariance determined and physiologically modelled gross primary production (Gpp) in a Douglas-Fir forest stand. Remote Sensing of Environment 107, 385–401.

Cox, P.M., Betts, R.A., Jones, C.D., Spall, S.A., Totterdell, I.J., 2000. Acceleration of global warming due to carbon-cycle feedbacks in a coupled climate model. Nature 408 (6809), 184–187. doi:10.1038/35041539.

Daly, E., Porporato, A., Rodriguez-Iturbe, I., 2004. Coupled dynamics of photosynthesis, transpiration, and soil water balance. Part I: upscaling from hourly to daily level. Journal of Hydrometeorology 5, 546–558.

Dang, Q.L., Margolis, H.A., Coyea, M.R., Sy, M., Collatz, G.J., 1997. Regulation of branch-level gas exchange of boreal trees: roles of shoot water potential and vapor pressure difference. Tree Physiology 17, 521–535.

Deming, D., 1995. Climatic warming in North-America – analysis of borehole temperatures. Science 268, 1576–1577.

Devito, K.J., Waddington, J.M., Branfireun, B.A., 1997. Flow reversals in peatlands influenced by local groundwater systems. Hydrological Processes 11, 103–110.

Devito, K., Creed, I., Gan, T., Mendoza, C., Petrone, R., Silins, U., Smerdon, B., 2005. A framework for broad-scale classification of hydrologic response units on the boreal plain: is topography the last thing to consider? Hydrological Processes 19, 1705–1714.

Eagleson, P.S., 1978. Climate, soil, and vegetation. 3. Simplified model of soil-moisture movement in liquid-phase. Water Resources Research 14, 722–730.

El Maayar, M., Chen, J.M., 2006. Spatial scaling of evapotranspiration as affected by heterogeneities in vegetation, topography, and soil texture. Remote Sensing of Environment 102, 33–51.

Environment Canada, 2006. Canadian climate normals or averages 1971–2000. <http://www.climate.weatheroffice.ec.gc.ca/climate_normals/index_1961_1990_e.html>.

Farquhar, G.D., Caemmerer, S.V., Berry, J.A., 1980. A biochemical-model of photosynthetic CO_2 assimilation in leaves of C-3 species. Planta 149, 78–90.

Friedlingstein, P., Cox, P., Betts, R., Bopp, L., Von Bloh, W., Brovkin, V., Cadule, P., Doney, S., Eby, M., Fung, I., Bala, G., John, J., Jones, C., Joos, F., Kato, T., Kawamiya, M., Knorr, W., Lindsay, K., Matthews, H.D., Raddatz, T., Rayner, P., Reick, C., Roeckner, E., Schnitzler, K.G., Schnur, R., Strassmann, K., Weaver, A.J., Yoshikawa, C., Zeng, N., 2006. Climate-carbon cycle feedback analysis: results from the (Cmip)-M-4 model intercomparison. Journal of Climate 19, 3337–3353.

Gale, M.R., Grigal, D.F., 1987. Vertical root distributions of northern tree species in relation to successional status. Canadian Journal of Forest Research – Revue Canadienne De Recherche Forestiere 17, 829–834.

Gedney, N., Cox, P.M., Betts, R.A., Boucher, O., Huntingford, C., Stott, P.A., 2006. Detection of a direct carbon dioxide effect in continental river runoff records. Nature 439, 835–838.

Govind, A., Chen, J.M., Margolis, H., Bernier, P.Y., 2006. Topographically driven lateral water fluxes and their influence on carbon assimilation of a black spruce ecosystem. EOS Transactions of AGU 87 (52) (Fall meet. Suppl., Abstract B23E-06).

Govind, A., Chen, J.M., Ju, W., in press. Spatially explicit simulation of hydrologically controlled carbon and nitrogen cycles and associated feedback mechanisms in a boreal ecosystem. Journal of Geophysical Research – Biogeosciences. doi:10.1029/2008JG000728.

Grant, R.F., 2004. Modeling topographic effects on net ecosystem productivity of boreal black spruce forests. Tree Physiology 24, 1–18.

Grant, R.F., Zhang, Y., Yuan, F., Wang, S., Hanson, P.J., Gaumont-Guay, D., Chen, J., Black, T.A., Barr, A., Baldocchi, D.D., Arain, A., 2006. Intercomparison of techniques to model water stress effects on CO_2 and energy exchange in temperate and boreal deciduous forests. Ecological Modelling 196, 289–312.

Heddeland, I., Lettenmaier, D., 1995. Hydrological Modeling of Boreal Forest Ecosystems. Water Resource Series. Department of Civil Engineering, University of Washington.

Heijmans, M.M.P.D., Arp, W.J., Chapin, F.S., 2004. Controls on moss evaporation in a boreal black spruce forest. Global Biogeochemical Cycles 18.

Hornberger, G.M., Bencala, K.E., Mcknight, D.M., 1994. Hydrological controls on dissolved organic-carbon during snowmelt in the Snake River near Montezuma, Colorado. Biogeochemistry 25, 147–165.

Hunt, E.R., Piper, S.C., Nemani, R., Keeling, C.D., Otto, R.D., Running, S.W., 1996. Global net carbon exchange and intra-annual atmospheric CO_2 concentrations predicted by an ecosystem process model and three-dimensional atmospheric transport model. Global Biogeochemical Cycles 10, 431–456.

Jackson, R.B., Canadell, J., Ehleringer, J.R., Mooney, H.A., Sala, O.E., Schulze, E.D., 1996. A global analysis of root distributions for terrestrial biomes. Oecologia 108, 389–411.

Jarvis, P.G., 1976. Interpretation of variations in leaf water potential and stomatal conductance found in canopies in field. Philosophical Transactions of the Royal Society of London Series B – Biological Sciences 273, 593–610.

Jenson, S.K., Domingue, J.O., 1988. Extracting topographic structure from digital elevation data for geographic information system analysis. Photogrammetric Engineering and Remote Sensing 54 (11), 1593–1600.

Ju, W.M., Chen, J.M., 2005. Distribution of soil carbon stocks in Canada's forests and wetlands simulated based on drainage class, topography and remotely sensed vegetation parameters. Hydrological Processes 19, 77–94.

Ju, W.M., Chen, J.M., Black, T.A., Barr, A.G., Liu, J., Chen, B.Z., 2006a. Modelling multi-year coupled carbon and water fluxes in a boreal aspen forest. Agricultural and Forest Meteorology 140, 136–151.

Kavvas, M.L., Chen, Z.Q., Dogrul, C., Yoon, J., Ohara, N., Liang, L., Aksoy, H., Anderson, M.L., Yoshitani, J., Fukami, K., Matsuura, T., 2004. Watershed environmental hydrology (WEHY) model based on upscaled conservation equations: hydrologic module. ASCE Journal of Hydrologic Engineering 9, 450–464.

Kavvas, M.L., Yoon, J., Chen, Z.Q., Liang, L., Dogrul, E.C., Ohara, N., Aksoy, H., Anderson, M.L., Reuters, J., Hackley, S., 2006. Watershed environmental hydrology model: environmental module and its application to a California watershed. ASCE Journal of Hydrologic Engineering 11, 261–272.

Kimball, J.S., White, M.A., Running, S.W., 1997. Biome-Bgc simulations of stand hydrologic processes for Boreas. Journal of Geophysical Research – Atmospheres 102, 29043–29051.

Kirchmann, H., Snall, S., Eriksson, J., Mattsson, L., 1999. Properties and classification of soils of the Swedish long-term fertility experiments: V. Sites at Vreta Kloster and Hogasa. Acta Agriculturae Scandinavica Section B – Soil and Plant Science 55, 98–110.

Letts, M.G., Roulet, N.T., Comer, N.T., Skarupa, M.R., Verseghy, D.L., 2000. Parametrization of peatland hydraulic properties for the Canadian land surface scheme. Atmosphere–Ocean 38, 141–160.

Leuning, R., 1997. Scaling to a common temperature improves the correlation between the photosynthesis parameters J(Max) and V-Cmax. Journal of Experimental Botany 48, 345–347.

Liu, J., Chen, J.M., Cihlar, J., Park, W.M., 1997. A process-based boreal ecosystem productivity simulator using remote sensing inputs. Remote Sensing of Environment 62, 158–175.
Liu, J., Chen, J.M., Cihlar, J., Chen, W., 2002. Net primary productivity mapped for Canada at 1-km resolution. Global Ecology and Biogeography 11 (2), 115–129.
Liu, J., Chen, J.M., Cihlar, J., 2003. Mapping evapotranspiration based on remote sensing: an application to Canada's landmass. Water Resources Research 39 (7).
Lundberg, A., Halldin, S., 1994. Evaporation of intercepted snow – analysis of governing factors. Water Resources Research 30, 2587–2598.
Mackay, D.S., Band, L.E., 1997. Forest ecosystem processes at the watershed scale: dynamic coupling of distributed hydrology and canopy growth. Hydrological Processes 11, 1197–1217.
Mcguire, A.D., Melillo, J.M., Randerson, J.T., Parton, W.J., Heimann, M., Meier, R.A., Clein, J.S., Kicklighter, D.W., Sauf, W., 2000. Modeling the effects of snowpack on heterotrophic respiration across northern temperate and high latitude regions: comparison with measurements of atmospheric carbon dioxide in high latitudes. Biogeochemistry 48, 91–114.
Molotch, N.P., Blanken, P.D., Williams, M.W., Turnipseed, A.A., Monson, R.K., Margulis, S.A., 2007. Estimating sublimation of intercepted and sub-canopy snow using Eddy covariance systems. Hydrological Processes 21, 1567–1575.
Neff, J.C., Asner, G.P., 2001. Dissolved organic carbon in terrestrial ecosystems: synthesis and a model. Ecosystems 4, 29–48.
Nemani, R.R., Keeling, C.D., Hashimoto, H., Jolly, W.M., Piper, S.C., Tucker, C.J., Myneni, R.B., Running, S.W., 2003. Climate-driven increases in global terrestrial net primary production from 1982 to 1999. Science 300, 1560–1563.
Porporato, A., D'odorico, P., Laio, F., Rodriguez-Iturbe, I., 2003. Hydrologic controls on soil carbon and nitrogen cycles. I. Modeling scheme. Advances in Water Resources 26, 45–58.
Potter, C., Klooster, S., De Carvalho, C.R., Genovese, V.B., Torregrosa, A., Dungan, J., Bobo, M., Coughlan, J., 2001. Modeling seasonal and interannual variability in ecosystem carbon cycling for the Brazilian Amazon region. Journal of Geophysical Research – Atmospheres 106, 10423–10446.
Price, A.G., Dunham, K., Carleton, T., Band, L., 1997. Variability of water fluxes through the black spruce (*Picea Mariana*) canopy and feather moss (*Pleurozium schreberi*) carpet in the boreal forest of Northern Manitoba. Journal of Hydrology 196, 310–323.
Price, J.S., Branfireun, B.A., Waddington, J.M., Devito, K.J., 2005. Advances in Canadian wetland hydrology, 1999–2003. Hydrological Processes 19, 201–214.
Quinn, P., Beven, K., Chevallier, P., Planchon, O., 1991. The prediction of hillslope flow paths for distributed hydrological modeling using digital terrain models. Hydrological Processes 5, 59–79.
Rawls, W.J., Brakensiek, D.L., Saxton, K.E., 1982. Estimation of soil–water properties. Journal of Transactions of the ASAE 25, 1316–1320, 1328.
Reichstein, M., Rey, A., Freibauer, A., Tenhunen, J., Valentini, R., Banza, J., Casals, P., Cheng, Y.F., Grunzweig, J.M., Irvine, J., Joffre, R., Law, B.E., Loustau, D., Miglietta, F., Oechel, W., Ourcival, J.M., Pereira, J.S., Peressotti, A., Ponti, F., Qi, Y., Rambal, S., Rayment, M., Romanya, J., Rossi, F., Tedeschi, V., Tirone, G., Xu, M., Yakir, D., 2003. Modeling temporal and large-scale spatial variability of soil respiration from soil water availability, temperature and vegetation productivity indices. Global Biogeochemical Cycles 17.
Roberts, J., 2007. The role of plant physiology in hydrology: looking backwards and forwards. Hydrology and Earth System Sciences 11, 256–269.
Running, S.W., Coughlan, J.C., 1988. A general model of forest ecossytem processes for regional applications I. Hydrological balance, canopy gas exchange and primary production processes. Ecological Modelling 42, 125–154.
Schwarzel, K., Renger, M., Sauerbrey, R., Wessolek, G., 2002. Soil physical characteristics of peat soils. Journal of Plant Nutrition and Soil Science – Zeitschrift Fur Pflanzenernahrung Und Bodenkunde 165, 479–486.
Shinozaki, K., Yoda, K., Hozumi, K., Kira, T., 1964a. A quantitative analysis of plant form. Pipe model theory. I. Basic analysis. Japan Journal of Ecology, 97–105.
Shinozaki, K., Yoda, K., Hozumi, K., Kira, T., 1964b. A quantitative analysis of plant form. Pipe model theory. II. Further evidences of the theory and its application in forest ecology. Japan Journal of Ecology, 133–139.
Sonnentag, O., Talbot, J., Chen, J.M., Roulet, N.T., 2007. Using direct and indirect measurements of leaf area index to characterize the shrub canopy in an ombrotrophic peatland. Agricultural and Forest Meteorology 144, 200–212.
Sonnentag, O., Chen, J.M., Roulet, N.T., Ju, W., Govind, A., 2008. Spatially explicit simulation of peatland hydrology and carbon dioxide exchange: influence of mesoscale topography. Journal of Geophysical Research – Biogeosciences 113.
Tague, C.L., Band, L.E., 2004. RHESSys: regional hydro-ecologic simulation system—an object-oriented approach to spatially distributed modeling of carbon, water, and nutrient cycling. Earth Interactions, 1–42.
Tombul, M., Akyurek, Z., Sorman, A.U., 2004. Determination of soil hydraulic properties using pedotransfer functions in a semi-arid basin, Turkey. Hydrology and Earth System Sciences 8, 1200–1209.
Turner, D.P., Ritts, W.D., Styles, J.M., Yang, Z., Cohen, W.B., Law, B.E., Thornton, P.E., 2006. A diagnostic carbon flux model to monitor the effects of disturbance and interannual variation in climate on regional NEP. Tellus Series B – Chemical and Physical Meteorology 58, 476–490.
Verstraeten, W.W., Veroustraete, F., Feyen, J., 2006. On temperature and water limitation of net ecosystem productivity: implementation in the C-Fix model. Ecological Modelling 199, 4–22.
Voinov, A.A., Fitz, H.C., Costanza, R., 1998. Surface water flow in landscape models: I. Everglades case study. Ecological Modelling 108, 131–144.
Wang, S., Grant, R.F., Verseghy, D.L., Black, T.A., 2001. Modelling plant carbon and nitrogen dynamics of a boreal aspen forest in class – the Canadian land surface scheme. Ecological Modelling 142, 135–154.
Way, D.A., Sage, R.F., 2008. Elevated growth temperatures reduce the carbon gain of black spruce (*Picea mariana* (Mill.) B.S.P.). Global Change Biology 14, 624–636.
Weiler, M., McDonnell, J.J., 2007. Conceptualizing lateral preferential flow and flow networks and simulating the effects on gauged and ungauged hillslopes. Water Resources Research 43.
Wigmosta, M.S., Vail, L.W., Lettenmaier, D.P., 1994. A distributed hydrology-vegetation model for complex terrain. Water Resources Research 30, 1665–1679.
Williams, T.G., Flanagan, L.B., 1998. Measuring and modelling environmental influences on photosynthetic gas exchange in *Sphagnum* and *Pleurozium*. Plant Cell and Environment 21, 555–564.
Wilson, K.B., Baldocchi, D.D., Hanson, P.J., 2001. Leaf age affects the seasonal pattern of photosynthetic capacity and net ecosystem exchange of carbon in a deciduous forest. Plant Cell and Environment 24, 571–583.
Winner, W.E., Thomas, S.C., Berry, J.A., Bond, B.J., Cooper, C.E., Hinckley, T.M., Ehleringer, J.R., Fessenden, J.E., Lamb, B., Mccarthy, S., Mcdowell, N.G., Phillips, N., Williams, M., 2004. Canopy carbon gain and water use: analysis of old-growth conifers in the Pacific Northwest. Ecosystems 7, 482–497.
Yu, G.R., Wang, Q.F., Zhuang, J., 2004. Modeling the water use efficiency of soybean and maize plants under environmental stresses: application of a synthetic model of photosynthesis–transpiration based on stomatal behavior. Journal of Plant Physiology 161, 303–318.
Zhou, X.L., Peng, C.H., Dan, Q.L., 2006. Formulating and parameterizing the allocation of net primary productivity for modeling overmature stands in boreal forest ecosystems. Ecological Modelling 195, 264–272.
Zhuang, Q., Melillo, J.M., Kicklighter, D.W., Prinn, R.G., Mcguire, A.D., Steudler, P.A., Felzer, B.S., Hu, S., 2004. Methane fluxes between terrestrial ecosystems and the atmosphere at northern high latitudes during the past century: a retrospective analysis with a process-based biogeochemistry model. Global Biogeochemical Cycles 18.
Zimov, S.A., Schuur, E.A.G., Chapin, F.S., 2006. Permafrost and the global carbon budget. Science 312, 1612–1613.